Method of Measuring Nitric Oxide Release by Vascular Endothelial Cells Grown in Microfluidic Channels

by

Shaghayegh Hosseinpour

B.Sc., Islamic Azad University of Science and Research of Tehran, 2003

Thesis Submitted in Partial Fulfillment of the
Requirements for the Degree of
Master of Applied Science

in the
School of Engineering Science
Faculty of Applied Sciences

SIMON FRASER UNIVERSITY

Fall 2014

Approval

Name: **Shaghayegh Hosseinpour**

Degree: **Master of Applied Science**

Title: ***Method of Measuring Nitric Oxide Release by Vascular Endothelial Cells Grown in Microfluidic Channels***

Examining Committee: **Chair:** Michael Sjoerdsma
Senior Lecturer, School of Engineering Science

Bonnie L. Gray, P. Eng
Senior Supervisor
Associate Professor

Andrew Rawicz, P. Eng
Supervisor
Professor

Glenn H. Chapman, P. Eng
Internal Examiner
Professor
School of Engineering Science

Date Defended/Approved: November 21, 2014

Partial Copyright Licence

Abstract

In this thesis, a simple and versatile method is developed which enables detection of nitric oxide (NO) released from vascular endothelial cells (ECs) cultured in microfluidic structures. The new culturing system and NO measurement method allow cell shape to be controlled in a non-invasive manner using microfluidic structures while NO release is monitored for cell shape versus function studies. The culturing system consists of arrays of polydimethylsiloxane (PDMS) fluidic channels 120 micrometers in depth and ranging from 100 micrometers to 3 mm in width. The number of channels in each array is varied to yield a constant cell culture surface area (75 mm^2) independent of channel width. The channel surfaces are collagen-coated and ECs are cultured to confluence within the channels. A cell scraper is then used to scrape extraneous cells cultured between channels, and NO measurements are made 18 to 24 hours later. A chemiluminescence-based sensor system (NOA 280i, Sievers NO Analyzer) is utilized to measure sample NO. Initial results indicate that NO concentrations can be measured from different microfluidic channel-containing samples using this method. Initial results suggest that there is no significant difference in NO concentration derived from channels of different widths even though the degree of cell elongation varies due to physical constraint by microfluidic channel walls. Cells treated with TNFα appear more elongated and release slightly more NO than untreated cells in fluidic channels; however, the ANOVA test indicates that this difference may not be significant for both microfluidic channels or fluidic channels and forms a basis for further study.

Keywords: endothelial cells, atherosclerosis, microfluidics, nitric oxide sensors, cell function, cell shape

To the memory of my beloved father, Reza Hosseinpour, whose encouragement and support was always priceless. He was looking forward to the completion of this thesis and my going back home. I wish he was here but I am glad he saw this process was very close to the completion. I miss him today and every day. Thank you for everything.

Acknowledgements

Foremost, I would like to express my sincere gratitude to my senior supervisor, Dr. Bonnie Gray for accepting me as her graduate student and her constant support, guidance and motivation. It would never have been possible for me to take this work to completion without her incredible support and encouragement.

I would like to thank my supervisor, Dr. Andrew Rawics for being the best mentor and for all the help and guidance from the first I entered to SFU.

Thank you to Dr. Glenn Chapman for generously agreeing to be on my committee.

Thanks to Dr. Pascal Nicolas Bernatchez, Dept. Anesthesiology, Pharmacology & Therapeutics, University of British Columbia/St. Paul's Hospital (Vancouver, Canada) for training on and access to their Sievers 280i Nitric Oxide Analyzer. I also thank Dr. Jonathon Choy from MBB department at SFU and his student Arthur Liu for the access to their lab and training on their equipments.

I would like to thank my wonderful parents, Zohreh and Reza, who have always loved me unconditionally. Without them I would never be here. I consider myself the luckiest in the world to have such a supportive parents, standing behind me with their love and support.

Last, but never least, I would like to thank my dear husband, Ali, who has been a constant source of support and encouragement during the challenges of graduate school and life. I am truly thankful for having you in my life.

Table of Contents

List of Tables

List of Figures

List of Acronyms

ANOVA	Analysis of Variance
ATP	Adenosine Triphosphate
BAEC	Bovine Aortic Endothelial Cell
CHD	Coronary Heart Disease
CVD	Cardiovascular Disease
DMEM	Dulbecco's Modified Eagle's Medium
DPBS	Dulbecco's Phosphate-buffered Salin
EC	Endothelial Cell
eNOS	Endothelial Nitric Oxide Synthase
FGF2	Fibroblast Growth Factor 2
HF	Hydro Fluoric Acid
IPA	Isopropyl Alcohol
MBB	Molecular Biology and Biochemistry
MEMS	Microelectromechanical Systems
MSPB	Multi-shear Perfusion Bioreactor
NIH	National Institutes of Health
NO	Nitric Oxide
SI	Shape Index
NOA	Nitric Oxide Analyzer
PDMS	Polydimethyl Siloxane
PIV	Particle Image Velocimetry
PMT	Photomultiplier Tube
PSIG	Pound Per Square Inch Gauge
RCA	Radio Corporation of America
Si	Silicon
VEGF	Vascular Endothelial Growth Factor
VEGFA	Vascular Endothelial Growth Factor A

Chapter 1.

Introduction

Microfluidics is the science of design and fabrication of devices that concern extremely small volumes of fluids, using structures (e.g., microfluidic channels, chambers, sensors) whose sizes are most easily measured in micrometers. The advent of new microfabrication techniques and materials has enhanced the performance of these microfluidic systems in biological research remarkably [1,2]. One important area in which microfluidics has had an enormous impact is the area of cell biology, offering new methods and instrumentation allowing study of single cells and groups of cells employing microfluidic channel-based devices [3,4,5].

One important application of microfluidics has been in the area of vascular science, which combines results from molecular and cell biology with *in vitro* models of blood vessels [6] and *in vivo* tests to bring development in vascular diseases treatment through study of the vascular endothelium. The vascular endothelium is the layer of Endothelial Cells (ECs) lining the inner surface of all blood vessels in the body. Dysfunction of the vascular endothelium is an important factor in major diseases such as atherosclerosis. ECs play an important role in vascular function through the release of various gases, ions, and compounds [7]. Nitric oxide (NO) is one of the gases released from ECs, which is proposed as one of the most important regulators of EC function [8]. It is established that the endothelium-derived relaxing factor, NO, is responsible for various physiological effects such as smooth muscle relaxation, non-specific immune response, modulation in neurotransmission, and inhibition of platelet activation, aggregation and adhesion [9]. The reduction in NO release is known as a major mechanism of EC dysfunction and may result in atherosclerosis [10]. Therefore, studying EC function and the factors that affect NO release is of interest to vascular researchers;

vascular function can be monitored in part through the endothelium's release of Nitric Oxide (NO).

Microfluidics offers new methods allowing study of ECs employing microfluidic-channel based devices [6]. Many studies have suggested that cell morphology may regulate the function of various cell types including ECs [11]. Furthermore, the shape of ECs can be altered via microfluidic channels or other microstructures, which may also have an effect on EC function. Microfluidic instrumentation has been previously used to study the shape versus function of vascular ECs grown in elongated shapes in microfluidic channels under both flow and no flow conditions [12,13,14]. ECs thus elongated may have a very different functional response from ECs whose elongation is induced using other methods such as flow-based shear stress [15,16], preferential attachment using patterned surface structures [17,18,19], or using chemical compounds [20]. Indeed, physical methods of cell shape control, such as using grooved surfaces or microfluidic channel confinement, have been suggested as powerful methods to non-invasively control EC shape for shape versus function studies [12,21,22]. One method to non-invasively control EC elongation for shape versus function studies is to culture ECs in microfluidic channels of different widths, resulting in greater cell elongation in microfluidic channels of smaller width [12]. However, EC shape and NO release are not often studied simultaneously. Thus, there is need to develop versatile instrumentation in order to understand the relationship between EC shape, function and NO release in order to provide invaluable insights into arterial disease mechanisms.

The main objective of this thesis is to design a simple, versatile, accurate method to measure the small NO concentrations produced from ECs cultured in small fluidic channels in response to mechanical or chemical stimuli, which provides the capability for a range of morphological and functional studies within microfluidic-based systems. In order to study the relationship between EC shape and the amount of NO released, a proof-of-concept microfluidic system is designed, fabricated, and tested in this thesis that successfully measures the small NO concentrations produced from ECs cultured in microfluidic channels of different widths under no flow conditions. This system consists of four arrays of microfluidic channels, which are designed to have the same culturing surface area with equal length and different widths in order to have approximately the

same number of cultured cells. The presented method is highly versatile since it does not involve integrated NO sensors and can be performed on virtually any microfluidic channel geometry after cell culture and confluence. It is very simple in terms of both microinstrumentation design and measurement method. It employs the NOA 280i Sievers NO Analyzer, which offers one of the most accurate and versatile detection systems for NO analysis and is considered to be the best method for NO detection by researchers worldwide [23,24]. Furthermore, the fabricated microfluidic system design has the capability of being altered to a flow-through system to study ECs under flow in future.

In summary this work presented in this thesis makes the following contributions to the field of microfluidics-based endothelial cell shape versus function studies:

1. A novel method is developed to successfully measure the small concentrations of NO released from ECs cultured in microfluidic channels.

2. A novel method is developed which enables the comparison of the NO concentrations produced from ECs cultured in microfluidic channels of different widths, which provides the capability for a range of morphological and functional studies of ECs.

3. A cell-scraping technique is developed solely for this thesis to ensure that the measurements and comparisons were performed on approximately the same number of cells, and for cells grown exclusively inside the channels.

4. The versatility of the system is investigated to show that multiple stimulants (e.g., microfluidic channel confinement and chemical stimulation) could be acted on the cells simultaneously.

The organization of this thesis is as follows: Chapter 2 gives general background for the thesis including ECs, atherosclerosis, and previous applications of microfluidics for NO measurements from cultured ECs. Chapter 3 covers the general design and fabrication of fluidic and microfluidic channels; experimental methods including culturing of ECs and NO measurement methods that were developed in order to use the chemiluminescence sensor; and experimental results on a single fluidic and single

microfluidic channel that establish the method's capabilities to measure NO produced by ECs in fluidic channels of different sizes. Chapter 4 covers the design and fabrication of a microfluidic system to measure NO in response to microfluidic channel confinement, along with the experimental methods and results using fluidic and microfluidic channels of different widths. Chapter 5 shows the experimental methods and results of NO measurement from ECs cultured in the microfluidic system in response to chemical stimuli. Finally, proposed future work and conclusions are discussed in Chapter 6 and 7.

Chapter 2.

Background and Motivation

This chapter covers a brief background of atherosclerosis disease and the importance of ECs and NO release in the vascular system. In addition, the applications of microfluidics in vascular research and a variety of NO sensing techniques used to detect NO production by ECs in response to stimuli, are introduced.

2.1. Endothelium and Atherosclerosis

Cardiovascular disease (CVD) is known as the most frequent cause of death in modern industrialized countries. For example, it causes 4.35 million deaths each year in Europe, and 35% of deaths in the United Kingdom [25]. In 2008 CVD accounted for 29% of all deaths in Canada [26].The main forms of CVD are coronary heart disease (CHD) and stroke. Atherosclerosis is the pathology that underlies CHD, which can be defined as a focal, inflammatory fibro-proliferative response to multiple forms of endothelial injury [25]. Atherosclerosis is the arterial disease in which an artery wall thickens, thereby causing focal plaques that restrict blood flow. Further dysfunction and damage of vascular cells may result in plaque rupture, which occludes blood flow to downstream tissues and is the main cause of myocardial infarction. This arterial disease is the leading cause of mortality in the western world [11]. Its dysfunction may also be related to stroke.

The endothelium is a monolayer of ECs which constitutes the inner cellular lining of the blood vessels (arteries, veins and capillaries) and the lymphatic system. Thus, the endothelium is in direct contact with the blood/lymph and circulating cells. The term “endothelium” was first introduced in 1865 by the Swiss anatomist, Wilhelm His [27]. The endothelial monolayer is recognized to be a predominant player in the control of blood

fluidity, platelet aggregation and vascular tone. EC shape varies across the vascular system, but they are generally thin and slightly elongated. Their dimension is about 50–70 μm long, 10–30 μm wide and 0.1–10 μm thick [28]. ECs are orientated along the axis of the vessel in the blood vessel wall so as to minimize the shear stress forces exerted by the flowing blood *in vivo* [29,30,16] and *in vitro* [31,32,33]. It has been shown that early atherosclerotic lesions develop preferentially in arterial regions where ECs are cuboidal, which means that they are not elongated and have a more rounded shape. Arterial regions with elongated ECs are largely resistant to the development of atherosclerosis [12]. However, the basis of the correlation remains unknown despite large efforts of researchers to determine the nature of the relation.

The endothelium plays an important role in vascular function through the release of soluble factors [7]. One of the most important factors released by ECs is nitric oxide (NO) [8]. NO is a free radical that reacts quickly with superoxide anions to form peroxynitrite, or is rapidly inactivated by oxyhemoglobin to form nitrate and methemoglobin. As a result, it has an *in vivo* half-life in tissues and physiological fluids of only a few seconds, which presents a considerable technical challenge to performing direct measurements [7,34,35,36,37]. Reduction in NO released from ECs has been proposed as a major mechanism of EC dysfunction and may result in atherosclerosis [10].

2.2. Applications of Microfluidics to Endothelial Cell Research

The effect of flow on EC phenotype (shape and orientation) and activation state has been studied for many decades [38]. Recently, microfluidic systems have been investigated as an alternative to many conventional macroscopic tools to study the biological characteristics of ECs that were not previously amenable to study [39]. Microfluidic technology has enabled studies of cell behaviours with precise and localized application of experimental conditions unreachable using macroscopic tools. Control of EC elongation has been previously done under flow or without flow using a number of different strategies. The methods of controlling EC elongation using microfluidics are divided to three main groups as described below:

1. Forcing the cells to grow in channels of a specified geometry:

Non-invasive shape control and functional studies of ECs have been done *in vitro* using microfluidic devices with varying channel widths within which ECs are cultured. The varying channel widths in these devices induce different degrees of EC elongation [12], yet also provide easy imaging of cell monolayers These designs have been developed using a number of different materials to realize the microfluidic channels, and include silicon-on-glass [12] or SU-8-on-glass [40] microfluidic channel platforms that allowed for a wide range of EC functional studies. Such studies include image analysis of EC shape and alignment in microfluidic channels under flow and static conditions, as well as detection of cytoskeletal arrangement via staining and electrical activity monitoring via patch clamping of ECs exhibiting different degrees of microfluidic channel-induced elongation. Figure 2.1 shows photographs of EC monolayers cultured in collagen-coated microfluidic channels of different widths under static (no flow) conditions to non-invasively control EC elongation [12]. As can be seen in the picture, the different degrees of elongation can be seen from the cells cultured in plain plastic slide, 215 μm, 105 μm, 75 μm, and 65 μm microfluidic channels. The extent of cellular elongation in the microfluidic channels was previously quantified by determining the shape index (SI), which is a dimensionless measure of cell roundness [12]. Figure 2.2 shows the change in SI of ECs cultured in microfluidic channels with width from 25 to 225 μm [12]. As can be seen, a significant elongation is shown in channels with width of less than 200 μm.

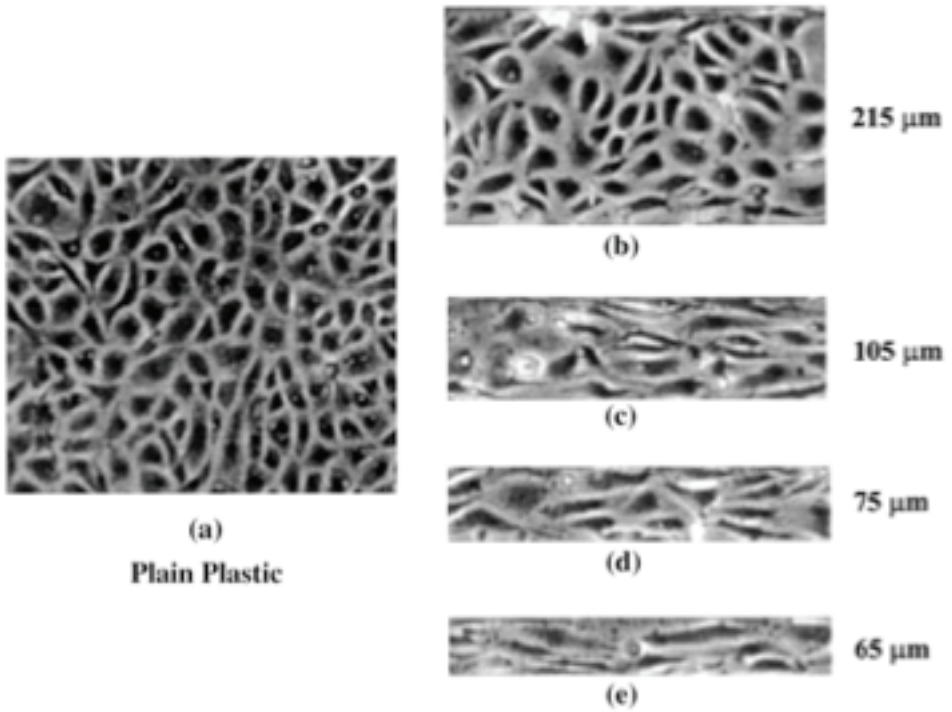

Figure 2.1 **Photographs of ECs, demonstrating increasing elongation with decreasing microfluidic channel width: cells cultured on a (a) plain plastic slide; (b) 215-μm-wide microfluidic channel; (c) 105-μm-wide microfluidic channel; (d) 75-μm-wide microfluidic channel; and (e) 65-μm-wide microfluidic channel [12] (used with permission from Springer with license number 3402690271719)**

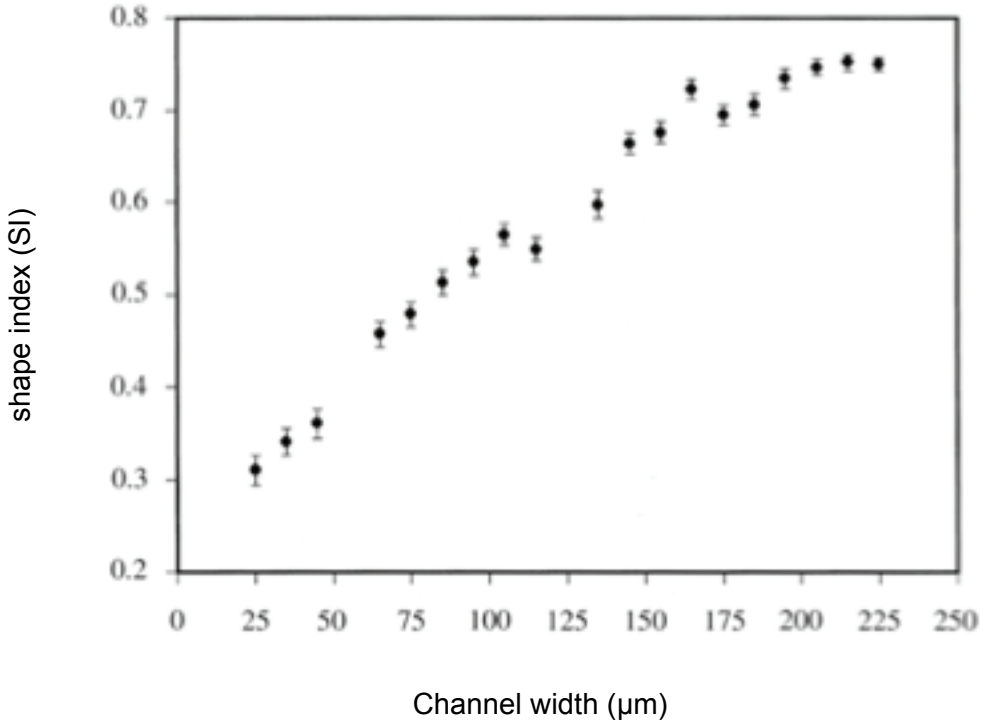

Figure 2.2 Shape index (SI) for ECs cultured in microfluidic channels as a function of microfluidic channel width [12]

Most of the fabricated microfluidic channels employed to study ECs have rectangular cross-sections [12,40], which do not replicate the circular cross-sections of blood vessels. However, an approach for the fabrication of microfluidic channels with circular cross-sections in polydimethylsiloxane (PDMS), using soft lithography [41], was also presented by a group of researchers who demonstrated the capability to grow endothelial cells on the inner surface of the microfluidic channels with circular cross-sections [42]. However, it should be noted that often rectangular cross-sectional microfluidic channels are chosen instead of circular cross-sectional channels due to the easier imaging of cells grown in such channels with flat surfaces.

2. Applying a controlled shear stress:

The mechanoresponse of ECs has been studied *in vitro* by subjecting ECs to shear stress in microfluidic devices. The EC monolayer's mechanoresponse, which is the biological response to mechanical stimuli, is proposed as a key factor in preventing atherosclerosis [6]. ECs line the inner lumen of blood vessels and so they are

continuously subjected to hemodynamic shear stress, which is known to modify EC morphology and biological activity. Therefore, most of the applications of microfluidics to the study of ECs involve investigation of the biochemical and mechanical response of individual ECs to different fluid dynamical conditions. Below are listed many examples of the applications of microfluidic devices in EC mechanoresponse research.

A multi-shear stress microfluidic device was introduced by a group of researchers which enabled the simultaneous evaluation of 10 different shear stresses ranging over two orders of magnitude to study EC mechanics and the influence of shear stress on EC morphology [43]. In a different study, Rossi, *et. al.*, fabricated a microfluidic flow chamber with a tapered geometry that created a pre-defined, homogeneous shear stress gradient on the EC layer [44]. A micro particle image velocimetry (micro-PIV) method, which is an optical method capable of measuring the velocity of fluid motion at microscopic scale with a spatial resolution of individual velocity measurements up to the sub-micrometer range, was used for the determination of the topography and shear stress distribution over cells with sub-cellular resolution. Another group of researchers described a self-contained microcirculatory EC culture system that efficiently studied the effects of shear stress on EC alignment and elongation *in vitro*. The culture system was composed of elastomeric microfluidic cell shearing chambers interfaced with computer-controlled movement of piezoelectric pins. The microfluidic culture system was integrated with microfluidic valves and pumps, which allowed one-step seeding of multiple EC shearing compartments that could then be re-circulated simultaneously in parallel but under different shear stress condition [45].

An integrated microfluidic cell culture chip was also presented in which ECs were under static (no flow) conditions or exposed to a pulsatile and oscillatory shear stress [46]. This microfluidic chip achieved multiple functions such as pulsatile and oscillatory fluid circulation, cell trapping, and cell culture through the integration of a microgap (interface between microchannels and microchambers in its design for cell trapping), self-contained flow loop, pneumatic pumps, and valves. The microfluidic chip enabled the study of the morphology and cytoskeleton of the ECs response to the pulsatile and oscillatory shear stress. In another study, a microfluidic mimic of the twisted channels in a modular tissue engineering construct enabled a detailed analysis of the effect of

disturbed flow patterns on EC phenotype. To study the flow through the irregular channels of a modular construct and to indicate its effect on the ECs that line them, a model modular construct was reproduced in a microfluidic circuit. The microfluidic system was used to create a “two-dimensional” mimic of the three dimensional flow in a construct [47].

3. Biochemical methods:

Another group of investigators used a novel microfluidic system to generate stable, spatially- and temporally- controlled gradients of the chemotactic factors vascular endothelial growth factor A (VEGFA) and fibroblast growth factor 2 (FGF2) to study EC migration in the context of angiogenesis [48]. An early and critical step in angiogenesis, or new blood vessel formation, is the directed migration of ECs. The researchers designed and fabricated a microfluidic device to examine the polarization and chemotaxis of ECs in response to quantified gradients of vascular endothelial growth factor (VEGF). The system was designed in a way to generate stable concentration gradients of biomolecules in a cell culture chamber while minimizing the fluid shear stress experienced by the cells [20]. EC migration is also an important process in the repair of damaged tissue. Meer, *et. al*., presented a microfluidic wound-healing assay for quantifying EC migration [49]. ECs were seeded in a 500-μm-wide microfluidic channel and a wound was generated in the cells’ monolayer after the cell monolayer became confluent. Pictures of fixed positions in the wounds were taken every hour. The closing of the wound over time was analyzed using NIH ImageJ image analysis software and so the ECs’ migration could be measured.

In addition to these examples, there are many other examples of microfluidic devices that have been designed and fabricated to study EC biology and their relation to atherosclerosis disease. However, it is important to note that none of these systems were designed to measure NO production in microfluidic channels, or to facilitate measurements in channels of varying widths and/or in the presence of chemical stimuli. Thus, there remains a need for instrumentation that is designed to facilitate such studies; in the next section, prior efforts to measure NO produced by ECs in microfluidic systems is discussed.

2.3. NO Measurement from Endothelial Cells in Microfluidic Systems

Microfluidic methods have been previously used to detect the production of NO released from ECs in response to chemical or mechanical stimuli by applying a variety of NO sensing techniques. These methods include integrated amperometric NO sensors, fluorescence microscopy, and Western blot detection of endothelial NO synthase (eNOS) expression, which correlates well with NO release [50,51,52,53,54]. In 2012, Rotenberg, *et. al.,* indirectly measured the NO production from ECs cultured in alginate scaffolds within a micro-fabricated multi-shear perfusion bioreactor (MSPB) that were subjected to different levels of shear stress [53]. Another group of researchers investigated the effect of homocysteine on NO release in ECs cultured in conventional culturing flasks [55]. Homocysteine is a thiol-containing amino acid and an independent risk factor for coronary artery vascular diseases such as atherosclerososis [55]. The effect of adenosine triphosphate (ATP) on NO production released from ECs cultured in microfluidic channels has been also studied by many researchers [51,52]. These devices enabled the detection of NO production, which was stimulated with ATP using concentrations that are similar to *in vivo* levels of ATP in the microcirculation system [52]. Letourneae, *et. al.*, has also studied the effect of Esterogen estradiol on the NO production by ECs using a three-dimensional microfluidic device [9].

While all of these systems have shown successful NO detection in microfluidic or larger fluidic channels, these prior systems involved either complicated sensor integration [50,51,54], indirect measurement of NO [53], or the use of equipment requiring direct optical access to the microfluidic channel network, resulting in less versatility due to the need for complicated or large-area fluidic channel networks [52]. Also, since many of these systems involved integrated sensors, the sensors are not capable of being transferred to another microfluidic system or being used with any microfluidic channel geometry after cell culture and moreover require much more complicated microfabrication techniques needed to place the integrated sensors in the system. Therefore, to provide more convenient measurement protocol, a simple, versatile and less complicated method is developed in this thesis using a conventional state-of-the-art sensor to measure the small NO concentrations produced from ECs

cultured in small fluidic channels. Direct NO measurement is done in this system that does not involve any complicated sensor integration, which makes it more versatile compared to the prior systems.

Existing systems do provide the ability to study the effect of many mechanical and chemical stimulants on NO production from ECs; such stimuli may include mechanical (e.g., shear stress) or chemical (e.g., ATP) stimulation of EC monolayers. However, the effect of microfluidic channel confinement on NO production has never been studied in microfluidic devices, although such studies could provide invaluable insights into atherosclerosis disease. The relationship between EC shape and NO release has not previously been studied simultaneously in microfluidic devices, nor has a method been previously developed whose goal is to provide a platform and measurement protocol for such studies.

2.4. Motivation for New Tool Development

To provide a new tool for vascular researchers, a simple and versatile method is developed in this thesis using a highly accurate sensor to measure the small NO concentrations produced from ECs cultured in small fluidic channels in response to mechanical and/or chemical stimuli. The presented method enables morphological and functional studies of ECs cultured within microfluidic channels of varying widths and thus enables the study of microfluidic channel confinement on NO production. Not having an integrated sensor makes this method very versatile and so it is capable of being used with any microfluidic channel geometry after cell culture. The method employs one of the most widely used sensors for the measurement of NO: the ozone based chemiluminescence method, which is highly sensitive with nanomolar detection limits [56]. In addition, the system presented in this thesis features a simple microfabrication process since there is no sensor integration and is very simple to use to obtain NO measurements from EC monolayers.

The basic system consists of four arrays of microfluidic channels, which are designed to have the same culturing surface area with equal length and different widths in order to have approximately the same number of cultured cells so the system enables

the study of the relationship between EC elongation and NO production from a similar number of cells cultured in microfluidic channels of varying width. A culturing protocol is developed such that frozen ECs are thawed in 37°C water and transferred to be seeded in a flask; as cells reach confluency, they are trypsinized to be passaged (subcultured) in a microfluidic channel array. After reaching confluency in the microfluidic channels, a method employing a cell scraper is developed to scrape the cells grown between the channels. A protocol for extracting NO-rich cell culture samples 24 hours later from the microfluidic channels using a micropipette is developed. Samples are transferred into an Ependorf safe-lock tube and then frozen until tested for NO concentration. Finally, an ozone-chemiluminescence-based sensor system is employed to detect and measure the amount of NO in samples and data is acquired with Liquid program.

Chapter 3.

NO Measurement Released from ECs Cultured in PDMS Microfluidic Channels

To ensure that the NO released from ECs cultured in PDMS microfluidic channels could be detected using the chemiluminescence sensor, ECs were first cultured on the surface of two differently sized single fluidic channels and a method to measure their NO production developed before extending the method to a more complicated multiple channel system. The design and fabrication of the fluidic channels, methods developed to culture ECs within the channels, and methods to detect their NO production, are discussed in detail in this chapter. The amount of NO released from ECs cultured in the single fluidic and single microfluidic channels as measured by the chemiluminescence sensor are also presented in this chapter as a proof-of-concept demonstration of the system.

3.1. General Design and Choice of Materials

Two fluidic channels, one larger channel and one microfluidic channel, were designed in order to develop a method of measuring NO from EC monolayers cultured in them and to determine if such a method could produce measurable results. A fluidic channel with dimensions of 4 mm, 28 mm, and 120 μm for fluidic channel width, length and depth, respectively, and microfluidic channel with dimensions of 0.7 mm, 6 mm, and 120 μm for fluidic channel width, length and depth, respectively, were designed and fabricated from Poly Di-Methyl Siloxane (PDMS). PDMS is a silicone elastomer that is widely used in microfluidics due to its inexpensive fabrication cost, flexibility, biocompatibility, and ease of fabrication. PDMS is chemically stable and can be used in a temperature range of -45 to 200 °C [57]. Like many silicones, PDMS provides a good surface for EC culture and proliferation [51,58]. A circular inlet and a circular outlet fluidic

port, each 7 mm in diameter, were placed at each end of larger fluidic channel. A 1 mm-diameter circular inlet and outlet fluidic port were also each placed at the end of the microfluidic channel.

3.2. Fabrication Process

PDMS channels (the fluidic and microfluidic channels) were fabricated using soft lithography fabrication techniques. Soft lithography involves a group of techniques for fabricating a defined structure on a master in a soft elastomer. This master consists of a bas-relief of photoresist (SU-8 in this work) on a silicon wafer, which serves as a mould for PDMS. Sylgard 184 Silicon Elastomer Kit from Dow Corning was used in this thesis. The kit contains two liquid parts: base and curing agent, that were used as-purchased.

The mould used to fabricate the PDMS microfluidic channels was developed from SU-8. SU-8 is a negative, epoxy type, near-UV photoresist, which has been specifically developed for ultra-thick, high-aspect-ratio structures such as found in microelectromechanical systems (MEMS) that can be fabricated using standard lithography equipment [59]. SU-8 photoresist is called negative as the areas exposed to light become cross-linked and so remain on the substrate during the development while the unexposed areas are removed away after development. SU-8 is sensitive to a wavelength of 400 nm and absorbs light shorter than 360 nm [60]. The SU-8 used in this thesis was from Microchem and was also used as-purchased. Various thicknesses of SU-8 from 2 μm to 200 μm can be spun on the substrate in a single coating [61]. SU-8 has been widely used as a mould for PDMS soft lithography [62,63]. The layout of the mould for the channels was designed using L-Edit CAD and so a dark field photo mask was generated to be the negative of the channels.

Figure 3.1 shows the fabrication process for the SU-8 mould. A <100> silicon (Si) wafer was used as the substrate, which was thoroughly cleaned with an RCA 1 clean (NH_4OH:H_2O_2: de-ionized water in 1:1:5 ratio) at 80°C for 10 minutes to remove any organics on the surface. The RCA 1 process was followed by a 5% HF dip for 30 seconds to remove any native silicon oxide (a).

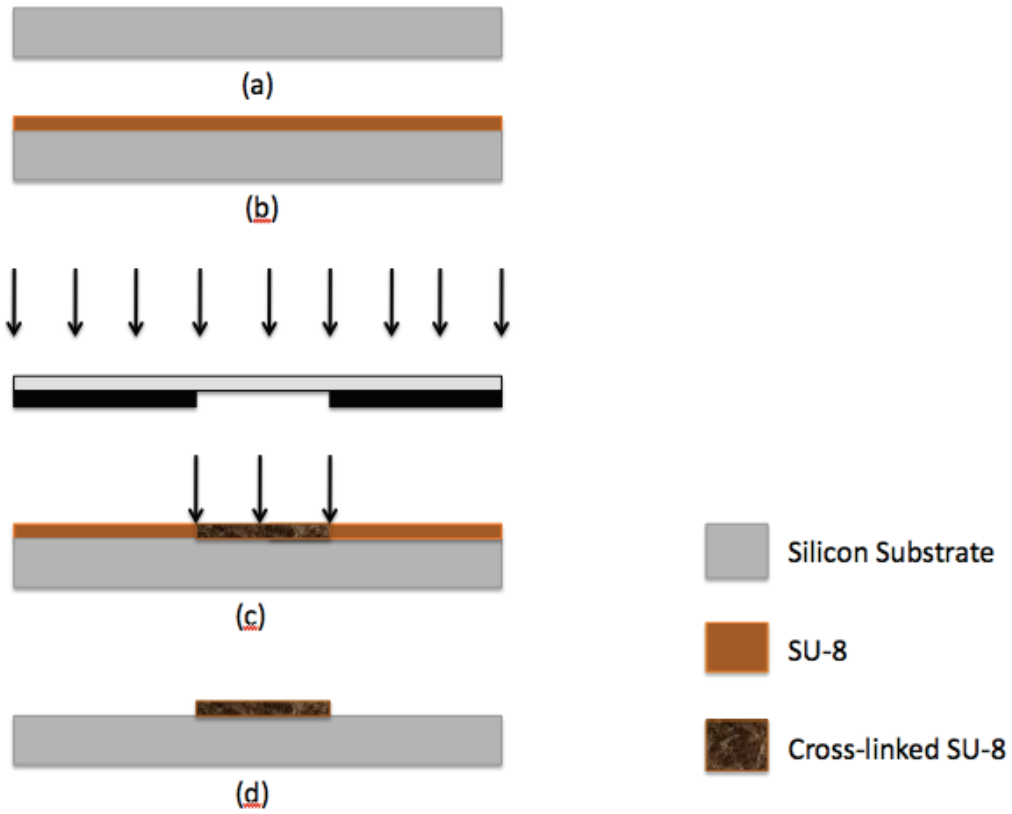

Figure 3.1 Fabrication process for 120 µm-thick SU-8 mould: a) clean the wafers; b) spin SU-8 photoresist and pre-bake; c) expose and post-exposure bake SU-8; d) develop.

As shown in Figure 3.1, SU-8 2035 was spun on the wafer at 1000 rpm for 30 seconds to create a 120 µm-thick layer (b). Pre-exposure soft bake was done at 65°C and 95°C for 5 minutes and 25 minutes, respectively. The SU-8 was then exposed with 260 mJ/cm^2 of UV light (wavelength of about 360 nm) for 15 seconds. SU-8 was then cross-linked during the post exposure bake at 65°C and 95°C for 5 minutes and 12 minutes, respectively (c). The layer of SU-8 was then developed using SU-8 Developer (Microchem) for 15 minutes (d). Any residual developer was washed away from the SU-8 mould using isopropyl alcohol (IPA). Figure 3.2 shows the fabricated SU-8 moulds for both fluidic channels and microfluidic channels from the perspective looking down on each mould.

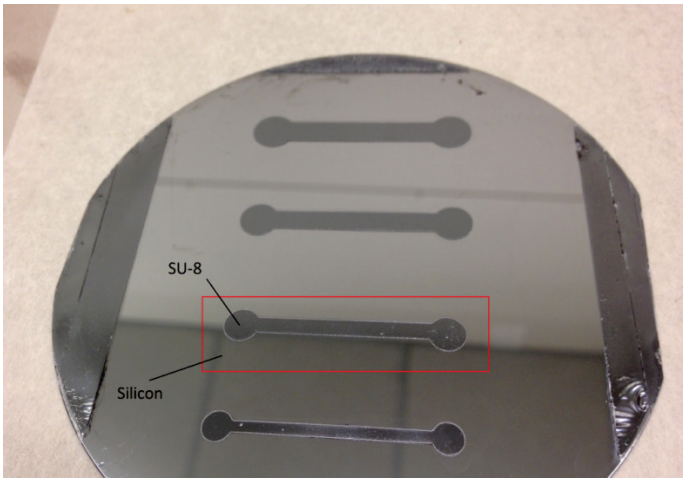

(a)

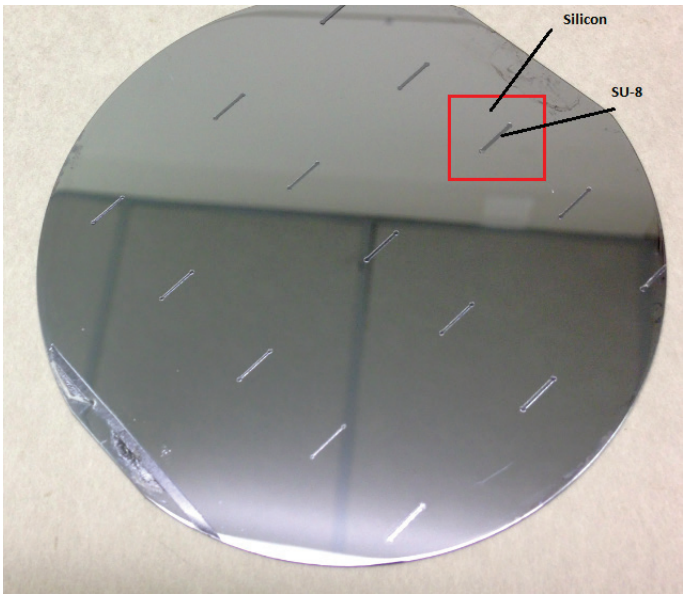

(b)

Figure 3.2 **The SU-8 moulds (looking down) of a) fluidic channels of different sizes (only the labeled 4 mm-width, 28 mm-length and 120 µm-depth channel was used in this work); and b) microfluidic channels of the same size (0.7 mm-width, 6 mm-length, and 120 µm-depth). Each silicon wafer is 100 mm in diameter.**

The soft-lithography-based fabrication sequence of the PDMS fluidic and microfluidic channels using the SU-8 mould masters is outlined in Figure 3.3. A thoroughly mixed liquid PDMS (10:1 mass ratio of base and curing agent, Dow Corning) was mixed and poured onto the mould master and the wafer was placed in a vacuum chamber for 20 minutes to eliminate trapped air bubbles (b). The wafer was then placed into an oven at 80°C for 60 minutes to cure the PDMS. Finally, the cured PDMS was peeled away from the substrate to create the fluidic/microfluidic channel arrays (f). The 4 mm-wide PDMS fluidic channel was manually cut into rectangular shape and placed on the surface of a Petri dish with diameter of 150 mm while the whole layer of PDMS containing 0.7 mm-wide microfluidic channels was placed on the surface of another same size Petri dish.

Figure 3.3 Fabrication process for PDMS fluidic and microfluidic channels: a) SU-8 mould fabricated using steps outlined in Figure 3.1; b) pour liquid PDMS onto the SU-8 mould; c) peel cured PDMS layer from substrate.

Both sets of PDMS channels and the inner and outer surfaces of the Petri dishes used for cell culturing were sterilized by spraying ethanol before starting the cell culture process. These were left on the biosafety cabinet for about 10 minutes to dry. The channels were then washed with Dulbecco's phosphate-buffered saline without calcium and magnesium (DPBS) for two times to remove the ethanol, which would kill the cells if not removed. The channels surfaces were then ready for cell culture.

3.3. Cell Culture

Bovine aortic ECs (BAECs) were employed because of their availability and close model to human ECs. BAECs were cultured in the channels by first coating the channels with collagen and then cell plating, as detailed in the following two sections. All collagen coating and cell plating had to be performed in a lab in Molecular Biology and Biochemistry (MBB) department under the direct supervision of the lab managers during normal business hour.

3.3.1. Collagen coating

The surface of the channels were coated with Type-I collagen from rat tail to enhance cell adhesion on the surfaces. Type-I collagen is the most common fibrillar collagen (90%), and is mostly found in skin, bones, tendons and other connective tissues. The collagen concentration of the stock as purchased was 3 mg/ml. However, the manufacture recommended concentration was 50 µg/ml, so the collagen had to be diluted 60 times in 0.02 M acetic acid. A starting concentration of 5 µg/cm^2 was also recommended by the manufacture for a thin coating process. The final volume of collagen and 0.02 M acetic acid was calculated using the following equations:

Equation 3-1

$$\text{Volume of collagen (V1)} = ((50\,\frac{\mu g}{ml}\ \text{of collagen}) \text{ x } (\text{Final volume}))/\ \text{Initial concentration of collagen } (\frac{\mu g}{ml})$$

Equation 3-2

$$\text{Volume of 20 mM acetic acid} = \text{Final volume} - \text{Volume of collagen (V1)}$$

The solution was added to both fluidic and microfluidic channels at 5 µm/cm^2 using micropipette. While the manufacture recommended to incubate the dishes at room temperature for one hour, better results were obtained when the dishes were left in a

heated incubator (95% air, 5% CO2 and) for 24 hours. After 24 hours the channels were washed with DPBS twice to remove the acetic acid.

3.3.2. Cell plating

A tube containing 1 ml of frozen BAECs (about one million cells) was thawed in a 37 °C water bath for 1 minute. The cells were then transferred to a flask and 20 ml of Dulbecco's Modified Eagle's Medium (DMEM, high glucose; Thermo Scientific) containing 4 mM L-glutamine, 4500 mg/l glucose, 1% penicillin + streptomycin, and 10% fetal bovine serum) was immediately added to the flask. The media had been warmed to 37 °C in advance. The flask was incubated for a few days and the media was renewed with fresh DMEM every 2 days.

After a few days the cells were confluent, attached as a monolayer on the surface of the flask and proliferated to millions of cells when checked under microscope. The media in the flask was discarded and the cells were washed with DPBS. In order to wash the cells, DPBS was first sprayed using a pipette gun to the surfaces where the cells were not attached and the flask was then shaken gently to move DPBS to wash all the cells. At the end the total fluid was extracted from one corner of the flask using a pipette gun and discarded.

Trypsin was used to cleave proteins bonding the cultured cells to the dish, so that the cells could be suspended in solution. The frozen trypsin was thawed in a 37 °C water bath before being added to the flask. The flask containing 3.5 ml of trypsin was incubated at 37 °C for 5 minutes and then 6.5 ml of fresh media was added to the flask. The total volume of fluid (10 ml) was then divided equally and transferred to two falcon tubes (5 ml each tube). The tubes were then centrifuged at 1500 RPM for 5 minutes to remove the trypsin and media. After being centrifuged, the cells were gathered at the tip of the tubes. The fluid containing the trypsin and media in each tube was then discarded in one step. The tubes were then tapped against the surface so the cells were detached from the tip of the tubes. One of the tubes was filled with 5 ml of fresh media and the whole content was then transferred to a new flask followed by adding 15 ml more of fresh media to the flask. The flask was labelled with the date, cells name, worker's name

and the passage number and left in the incubator to be used for later experiments. The cells are considered to be “passaged” once trypsinized, detached from the surface, and transferred to a new flask, and must be accounted for as cell lines deteriorate after a large number of passages. The second tube was filled with 4 ml of fresh media and used to fill a fluidic channel and seven sample microfluidic channels.

Since the volume of the fluidic channel (22.4 µl) and microfluidic channel (0.693 µl) were significantly less than the required volume (minimum 100 µl) needed to be collected for testing with the sensor, silicone isolators (Grace Bio-Labs) were used to make a barrier around each fluidic and microfluidic channel in order to provide a larger volume of fluid (550 µl and 50 µl for fluidic and microfluidic channels respectively). A rectangular shaped silicone isolator with rectangular cut-out was used around each fluidic channel and had dimensions of 4.8 x 2.3 cm and a depth of 0.5 mm. A rectangular shaped silicone isolator with circular cut-out was used around each microfluidic channel. Figure 3.4 shows a photograph of silicone isolators with a circular cut-out diameter of 9 mm used around the microfluidic channels.

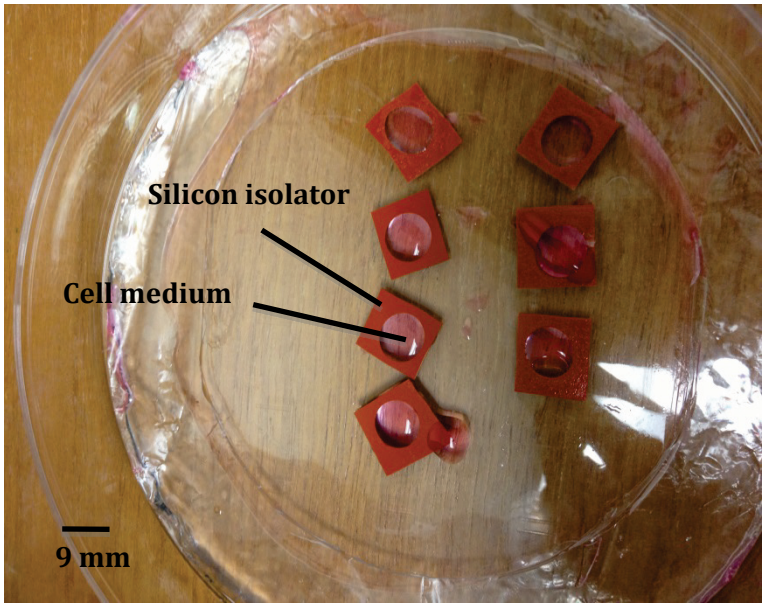

Figure 3.4 **Silicone isolators used to seal and create barriers around the microfluidic channels. The cell medium is the pink fluid shown covering each of the microfluidic channels inside the circular-shaped barriers. The culturing dish diameter is 150 mm.**

Figure 3.5 shows a photograph of ECs cultured within the single fluidic channel with dimensions of 4 mm, 28 mm, and 120 μm as width, length and depth, respectively, 24 hours after cells plating. A healthy confluent monolayer can be seen. Figure 3.6 also shows a photograph of ECs cultured within the microfluidic channels with dimensions of 0.7 mm, 6 mm, and 120 μm for fluidic channel width, length and depth, respectively. A healthy confluent monolayer can also be seen for ECs cultured in this microfluidic channel.

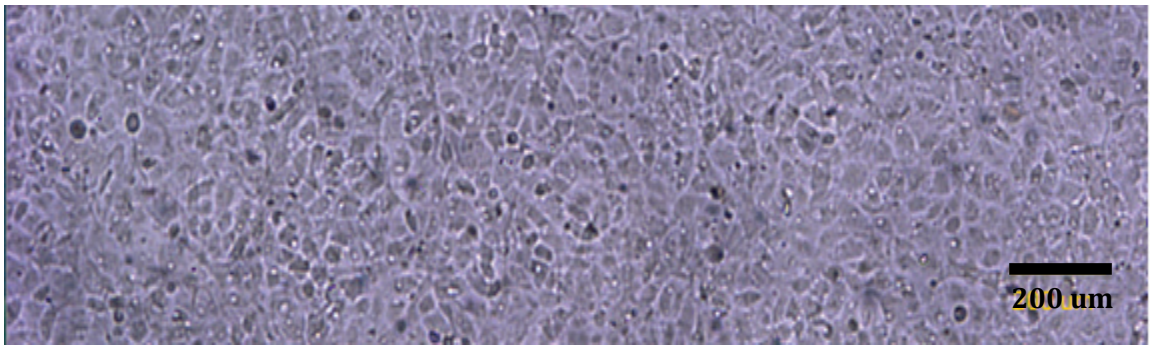

Figure 3.5 **Photograph of ECs cultured inside a fluidic channel sized: 4 mm-wide, 28 mm-long, and 120 μm-deep. This photograph was taken 24 hours after cell plating [64].**

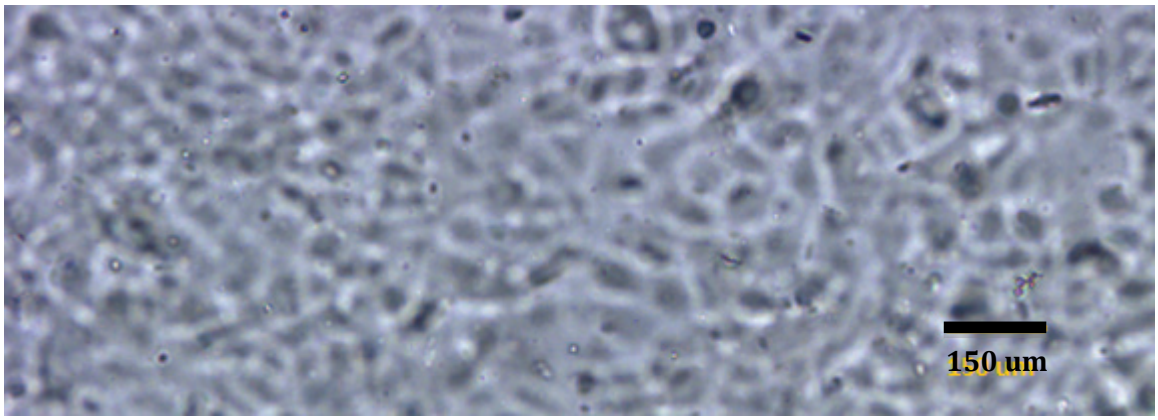

Figure 3.6 **Photograph of ECs cultured inside a microfluidic channel sized: 0.7 mm-wide, 6 mm-long, and 120 μm-deep. This photograph was taken 24 hours after cell plating.**

After the 24 hour cell plating period, approximately 500 μl of medium was collected from the fluidic channel using a micropipette and transferred into an Ependorf safe-lock tube. Approximately 150 μl of fluid in total was also collected from the seven

microfluidic channels and transferred to another Ependorf safe-lock tube. Since there was some evaporation, the total volume collected from the seven microfluidic channels (150 µl) was less than the volume initially added to the microfluidic channels (350 µl). Both Ependorf safe-lock tubes containing the sample fluids were then centrifuged to remove cellular debris and then stored at -80 ^{o}C until tested for NO concentration.

3.4. Chemiluminescence Detection of NO

An ozone-chemiluminescence-based sensor system (NOA 280i, Sievers Nitric Oxide Analyzer) was utilized in this work to detect and measure the amount of NO in each sample as it offers the most versatile detection system for NO analysis. Using this sensor we developed a simple protocol for measurements from microfluidic structures. The Sievers Nitric Oxide Analyzer (NOA 280i) is capable of measuring NO and its reaction products (nitrite, nitrate and nitrosothiols) in virtually any biological fluid including: cell culture media, plasma, sera, urine, cerebral-spinal fluid, bronchial-alveolar lavage, perfusates, and tissue homogenates [65]. The operating specification of Sieviers NO analyzer for liquids is presented in Table 3.1.

The Sieviers NO analyzer employed for the experiments in this work was located at UBC James Hogg research centre in St. Paul's hospital (Vancouver, Canada). The lab was supervised by Dr. Pascal Bernatchez whose research program elaborates new therapeutic avenues for human pathologies caused by blood vessel disorders, such as endothelial dysfunction, atherosclerosis, vascular inflammation. Due to the large demand of the sensor by the researchers in Dr. Bernatchez's lab and the necessity of supervision by the lab technicians, I had a limited access to the sensor and had to book the sensor at least two weeks in advance. Thus, as many samples as possible were collected during each access time. Another challenge encountered was carrying the frozen samples from the lab in MBB department, where the cells were plated and stored, to St. Paul's hospital. The samples had to remain cooled in a cooler containing the samples with dry ice.

Table 3.1 Operating specification of Sieviers NO analyzer [64]

Sensitivity	~1 picomole
Range	Nanomolar to millimolar
Response time	Electronics: 67 milliseconds to 90% full scale Lag Time: 1 second
Sample size	0.001-5 ml
Repeatability	± 5–10%
Display	Back-lit LCD screen
	ppb/ppm or mV
Outputs	Analog: 0-1V, 0-10V
	Digital: RS-232 (9600-38.4K baud)
	Printer: Parallel port
Data sampling rate	0.002–32 samples/second
Power requirements	120V, 60 Hz (6A)
	100V, 50 Hz (3A)
	230V, 50 Hz (3A)
NOA	Height: 16 in (41 cm)
	Width: 6.2 in (16 cm)
	Length: 20 in (51 cm)
	Weight: 35 lbs (16 kg)
Vacuum pump with installed trap	Height: 14.5 in (37 cm)
	Width: 7.5 in (19 cm)
	Length: 19 in (48 cm)
	Weight: 47 lbs (21.5 kg)

3.4.1. Principle of chemiluminescence measurement

The ozone chemiluminescence NO measurement relies on the reaction of NO with ozone (O_3) in a reaction cell to produce excited-state nitrogen dioxide (NO_2*), which emits light upon relaxation to the ground state as follows:

$$NO+O_3 \rightarrow NO_2^*+O_2$$

$$NO_2^* \rightarrow NO_2+h\nu$$

The NO/O_3 reaction emits light at wavelengths greater than 600 nm, which allows the use of a simple filter to remove undesirable signal and to impart complete selectively for NO [66]. The photons from this reaction are detected and transformed into an electrical signal by a photomultiplier tube (PMT). The current from the PMT is A/D converted and fed into a PC running dedicated software (Sievers NO Analysis Liquid Program).

The employed ozone-based chemiluminescence NO detector uses argon as an inert gas to deoxygenate the sample solution and carry gaseous NO into a reaction cell, where it reacts with O_3 generated from O_2 from a dedicated oxygen tank. The major advantage of employing a carrier gas is that the most troublesome interferents (e.g., NO_2^- and NO_3^-) are not transferred from the sample vessel to the reaction cell; thus, NO selectivity is enhanced [66].

The amount of light produced by NO/O_3 chemiluminescence is proportional to the amount of NO sampled. Hence, the calculated area under the curve of the PMT current for each determination is proportional to the amount of NO. This was verified before each experiment by standard curves (5, 10, 25 pmol) which were produced using freshly prepared solutions of 0.1 M sodium nitrite ($NaNO_2$).

3.4.2. Materials

Working with the sensor, several pieces of equipment and reagents were needed as follows:

Equipment

1. Nitric Oxide Analyzer: Sievers model 280i obtained from GE Analytical Instruments and located in UBC James Hogg research centre at St. Paul's Hospital
2. Liquid program (the title of the computer program is "Liquid")
3. Oxygen and inert gas (argon)
4. Syringe with capacity of minimum 5 µl and maximum 100 µl
5. Vortex mixer

Reagents

1. Distilled Water

2. 4.5 ml glacial acetic acid

3. 500 µl of 10% sodium iodide (NaI), which is prepared by dissolving 0.1 g NaI in 1 ml distilled H_2O

4. Standard solution: 10^{-6} M sodium nitride ($NaNO_2$), which is freshly prepared every time the sensor is used as follows:

   A. Preparing 1 M sodium nitride ($NaNO_2$) by dissolving 0.069 g $NaNO_2$ in 1 ml H_2O
   B. Diluting the 1 M solution to 10^{-2} M solution by adding 10 µl of 1 M solution to 990 µl of water
   C. Diluting the 10^{-2} M solution to 10^{-4} M solution by adding 10 µl of 10^{-2} M solution to 990 µl of water
   D. Diluting the 10^{-4} M solution to 10^{-6} M solution by adding 10 µl of 10^{-4} M solution to 990 µl of water

3.4.3. Analyzer start-up and calibration of chemiluminescence

The NO analyzer is kept in a room at a stable temperature. After turning on the vacuum pump, the vacuum must reach a stable 8 torr level before use. The argon and oxygen gas valves, which are located directly above the gas tanks, may then be opened. The supply pressure (oxygen) has to be adjusted to 5.8-6.2 PSIG with a black knob located behind the NO analyzer.

For the experiments presented here, 4.5 ml of glacial acetic acid and 500 µl of 10% NaI was added inside the purge column. Once the baseline was stabilized, volumes of 5 µl, 10 µl, and 25 µl of the working standard solution (10^{-6} M $NaNO_2$) were injected into the purge vessel in triplicates using a syringe so that the chemiluminescence signals could be recorded. Note that the syringe was rinsed at least five times between injections.

A software program, called the Liquid program, is used to acquire data. The NO analysis is a suite of four programs (Liquid, REB, Bag and Breath) for collection and processing of data . Data is collected via the computer serial port and the programs can be run on a PC. All files are saved in a tab-delimited text format for easy import into a spreadsheet or statistics programs [65]. The Liquid program is used with the purge vessel to acquire data, name the samples, integrate the peaks (using threshold and peak width detection and automatic select of start and stop integration marks), prepare calibration curves, calculate the concentration of the samples and save the results. The software also calculates the area under the curve. It should be noted that a new standard curve is generated from the standard solution each time that measurements are made, and this curve is then used to calculate NO concentration from test samples. For the work here, the average of the three values from three same injections were calculated and data from these injections was used to generate standard curves in Microsoft Excel. Figure 3.7 shows the experimental set up for the chemiluminescence NO measurement using the NOA 280i analyzer.

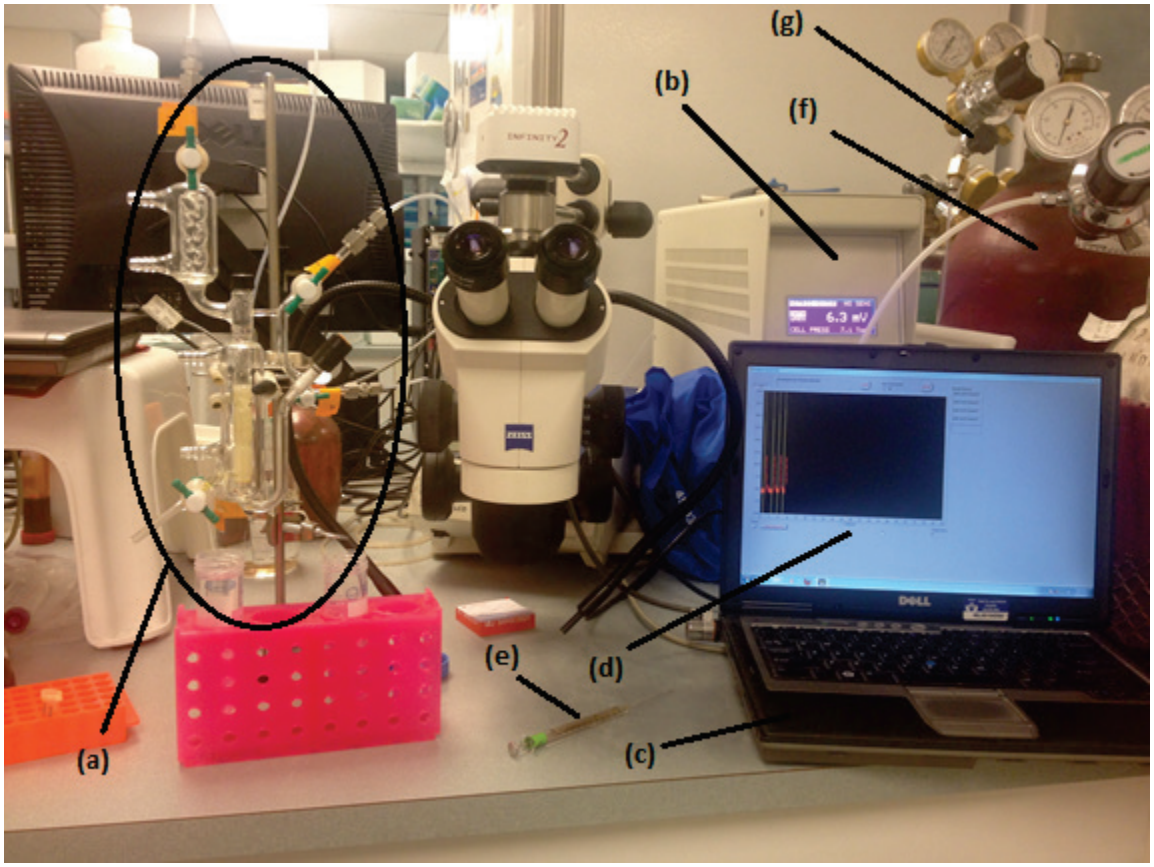

Figure 3.7 **A photograph of the equipment used for chemiluminescence NO analysing: a) purge vessel; b) NOA 280 i analyzer; c) PC; d) Liquid program; e) syringe; f) oxygen tank; g) argon tank**

A negative control must be done whenever the machine is used, which means measuring the signal from DMEM only, so the net value for the samples can be calculated later by subtracting the value of DMEM only from the sample values.

For the experiments performed in this thesis, the previously frozen samples were kept in an ice box until injected. They were taken out of the ice box a few minutes before injections, thawed in the water bath, and mixed using a vortex mixer prior to analysis. NO-rich cell culture samples were then injected into the machine in triplicate (20 µl each time). The average value of the three results from the same samples was calculated and the final results (NO concentration) were calculated using the standard curve. The concentration of NO is obtained using the following equation:

Equation 3-3

$$[NO]\ \text{nM} = (\text{Average area} - \text{Y-intercept})/(\text{slope} \times \text{volume of sample injected})$$

3.5. Experimental Results

The results from chemiluminescence NO detection of each sample was calculated using the standard curve and with Microsoft Excel. Figures 3.8 and 3.9 show the data from standard solution and NO-rich cell culture samples injections, respectively, which were provided with Liquid software. Figure 3.10 shows the calculation done in Microsoft Excel to find the NO concentration for both samples.

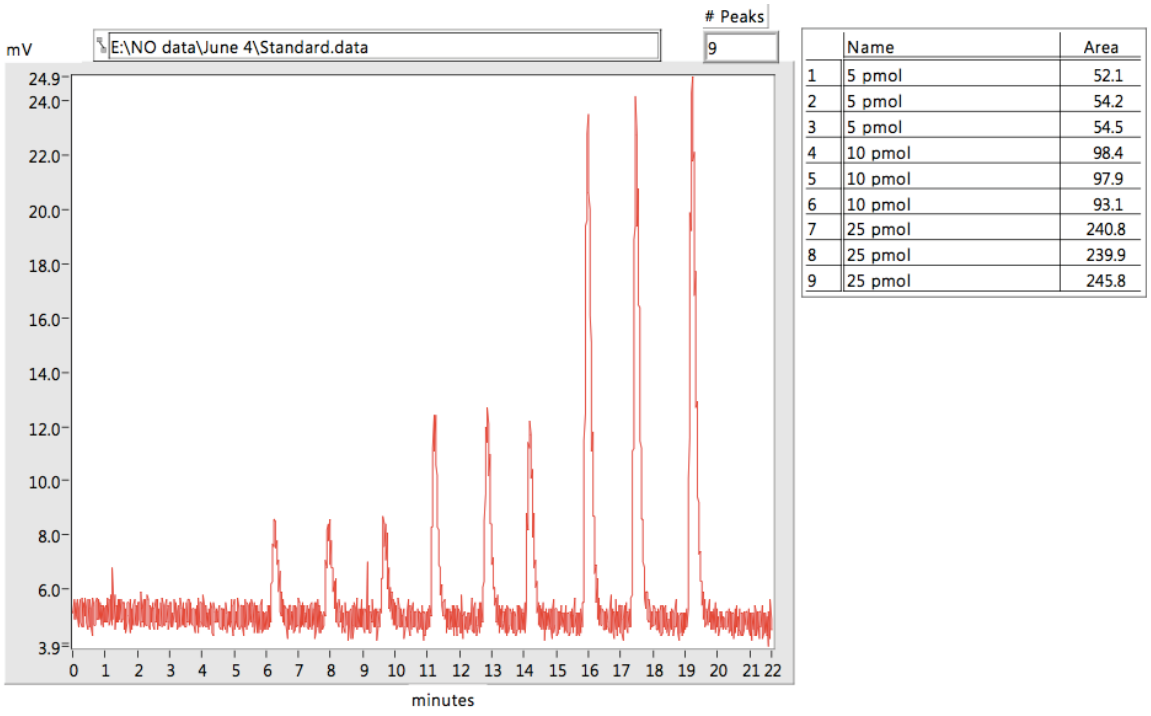

	Name	Area
1	5 pmol	52.1
2	5 pmol	54.2
3	5 pmol	54.5
4	10 pmol	98.4
5	10 pmol	97.9
6	10 pmol	93.1
7	25 pmol	240.8
8	25 pmol	239.9
9	25 pmol	245.8

Figure 3.8 Plot of NO chemiluminescence signals obtained from the Liquid program after injections of 5, 10, 25 µL of *standard solution* (10^{-6} M sodium nitrite) in triplicate. The x-axis is time in minutes; the y-axis is photomultiplier current in mV. The table shows the area under each curve after each injection. The # peaks show the number of injections.

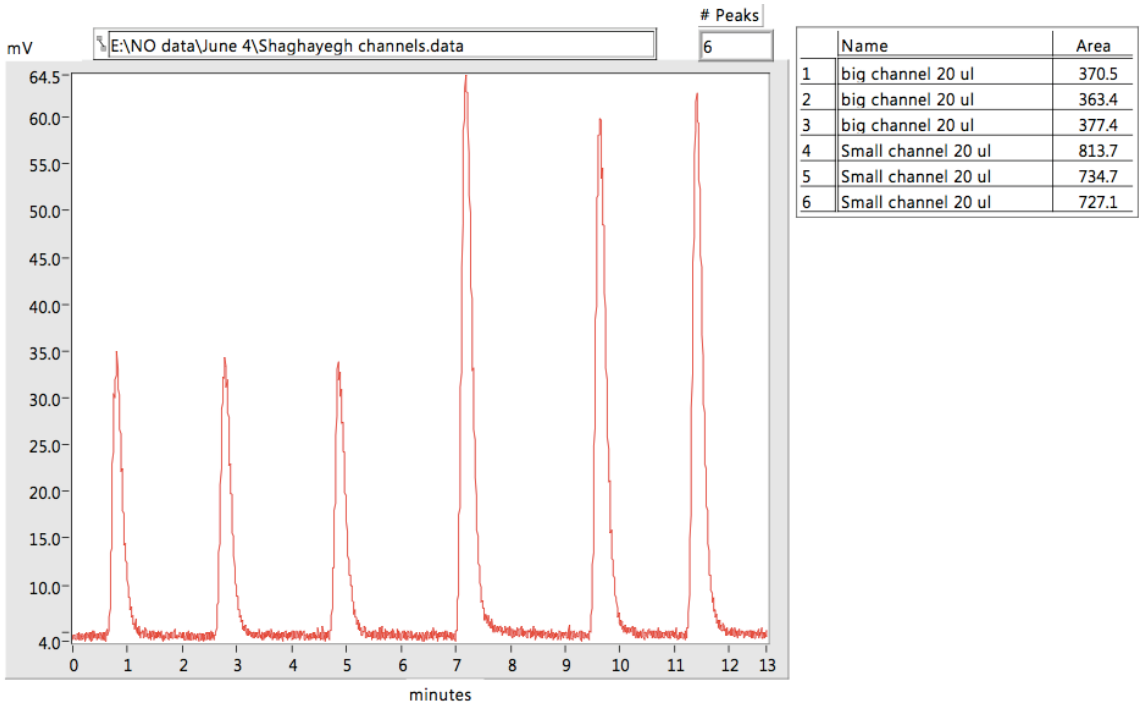

	Name	Area
1	big channel 20 ul	370.5
2	big channel 20 ul	363.4
3	big channel 20 ul	377.4
4	Small channel 20 ul	813.7
5	Small channel 20 ul	734.7
6	Small channel 20 ul	727.1

Figure 3.9 **Plot of NO chemiluminescence signals obtained from the Liquid program after injections of *NO-rich samples* in triplicate (6 injections total). The x-axis is time in minute; the y-axis is photomultiplier current in mV. The table shows the area under each curve after each injection. The # peaks show the number of injections.**

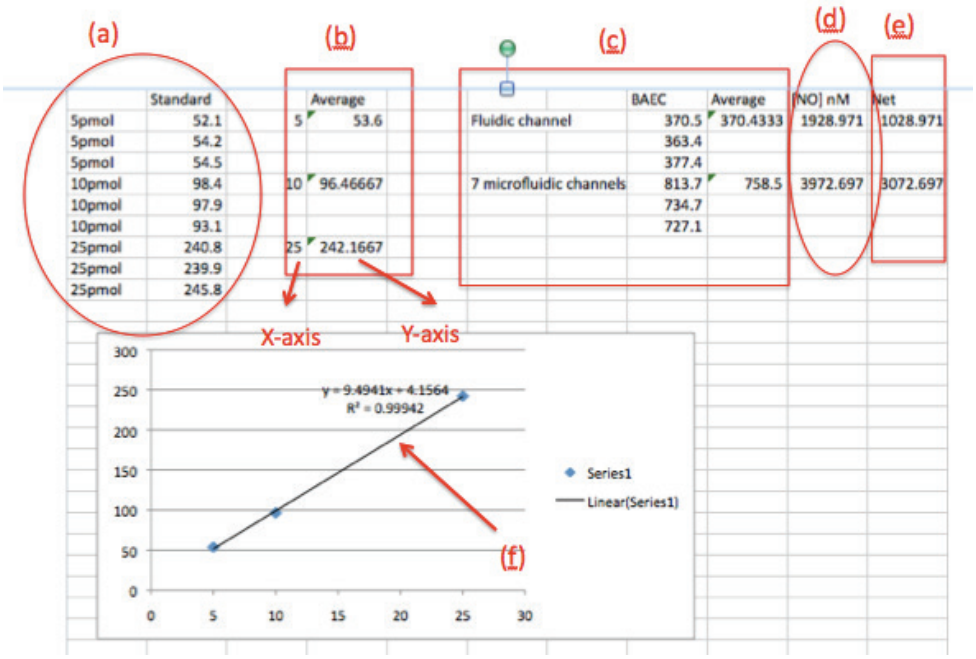

Figure 3.10 The Microsoft Excel program developed by the author to find the NO concentration of the samples: a) data from standard solution injections acquired with the Liquid program; b) data used to provide the standard curve; c) data from NO-rich sample injections acquired with the Liquid program; d) NO concentration; e) NO concentration above value of cell medium only; f) standard curve provided using data in (b).

As seen in the Figure 3.10, the cells cultured in the single 4 mm-wide fluidic channel produced an NO concentration of 1028.97 nM above values of cell medium alone (see column labelled (e)). The cells cultured in the seven 0.7 mm-wide microfluidic channels produced NO concentration of 3072.69 nM above values of cell medium alone. Dividing this value by the number of the microfluidic channels (7) gives an NO concentration of 438.95 nM from the cells cultured in only one microfluidic channel. These numbers indicate that the NO produced by cells in the fluidic channel or microfluidic channels were indeed measurable using the outlined methodology.

Chapter 4.

Microfluidic Culturing System for NO Measurement in Microfluidic Channels With Different Widths

In Section 2.2, it was discussed how previous studies have shown that geometric control of EC shape and orientation without flow can be obtained by culturing ECs in microfluidic channels of different widths. However, the effect, in any, on NO production in ECs grown in microfluidic channels of different widths has never been investigated before. Others have shown detection of NO in microfluidic channels [51,52], but in all cases that could be found in the literature, differences in NO concentration between various experiments, rather than absolute values of NO concentration, could only be found. In addition, the application of shear stress at levels producing elongated cells was found to increase NO production [53]. Again, no absolute value were given, so the increase in NO concentration (e.g., 350 nM) cannot be compared to baseline values. In this chapter, a simple and versatile method is presented to measure the small NO concentrations produced from ECs cultured in small fluidic channels with different widths to provide the capability for a range of morphological and functional studies within microfluidic-based systems that include NO detection.

4.1. Design and fabrication of microfluidic culturing system for NO measurement

The microfluidic cell culturing system consisted of four microfluidic channel arrays with equal length (2.5 cm) and depth (120 μm) but with varying widths of 100 μm, 200 μm, 300 μm, and 3 mm. Previous work has shown that elongation occurs for cells grown in microfluidic channels less than 200 μm wide (Figure 2.2). Thus, the four widths of fluidic channels (100 μm, 200 μm, 300 μm, and 3 mm) were chosen in order to provide elongated cells in the smallest channel, with no elongation in the largest channel

(3 mm channel), and a smaller degree of elongation for the other two channels (200 μm and 300 μm). Although smaller width channels could be used (e.g., 50 μm), smaller channels have been previously shown to be difficult for the culture of complete cell monolayers. Thus, the range of channel widths chosen covers a range of different degrees of elongation, while providing easy experimentation. In order to compare the NO release from a similar number of cells in each array, the samples were designed to have the same culturing surface and the same volume of cell medium (3 ml) for each array. The number of microfluidic channels in each array was varied to provide the same culturing surface area; for example, thirty 100 μm-wide microfluidic channels, as compared to one 3 mm-wide channel. Table 4.1 shows the number of channels with their dimensions for each array, which are numbered 1 through 4, where array 4 has the widest channel size (3 mm). Figure 4.1 shows the different designs (arrays 1 through 4) from a perspective looking down on the fluidic channels.

Table 4.1 Dimensions and number of channels for different microfluidic channel arrays[64]

Array #	Number of channels in array	Depth of channels (μm)	Length of channels (mm)	Width of channels (μm)	Culturing surface (mm^2)
1	30	120	25	100	75
2	15	120	25	200	75
3	10	120	25	300	75
4	1	120	25	3000	75

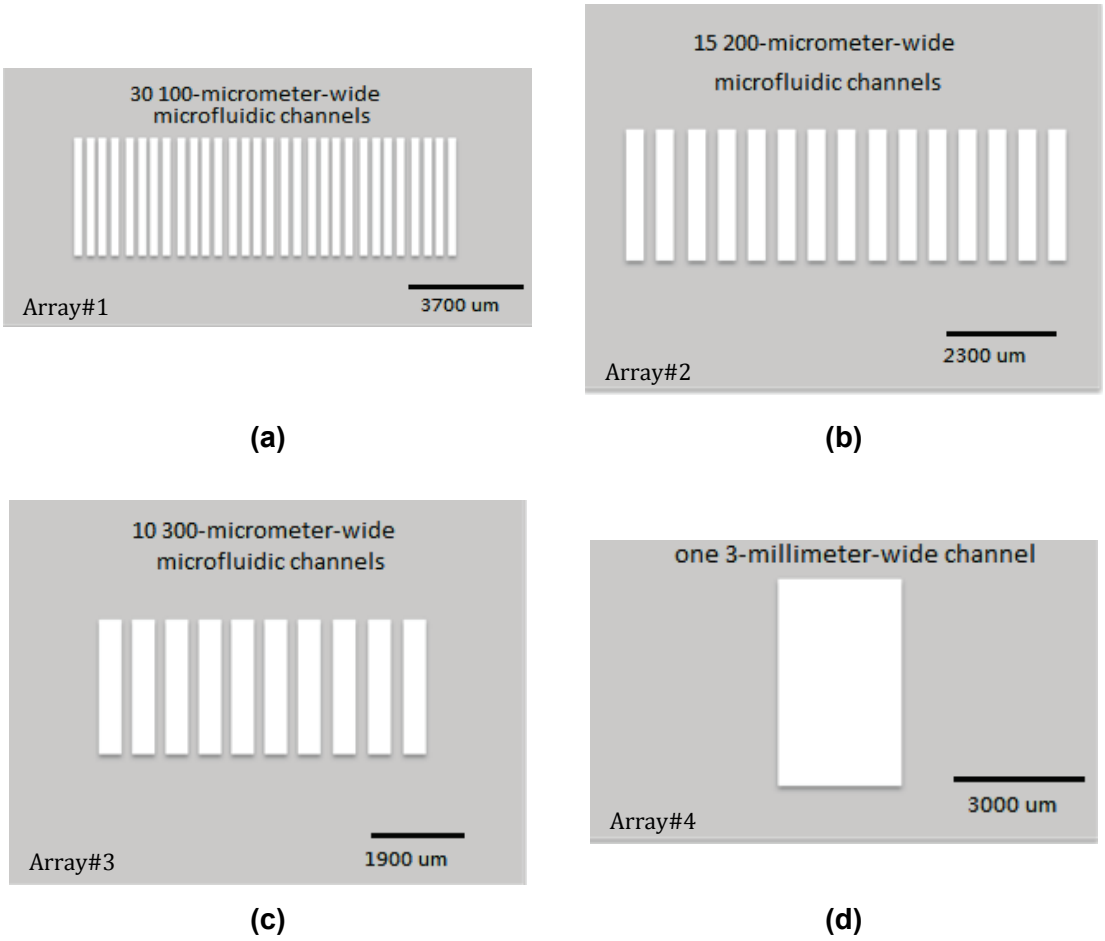

Figure 4.1 **The layout design (looking down) of four different channel arrays with the same channel culturing surface (75 mm2): a) 30 100 µm-wide microfluidic channels (Array #1); b) 15 200 µm-wide microfluidic channels (Array #2); c) 10 300 µm-wide microfluidic channels (Array #3); d) one 3 mm-wide fluidic channel (Array #4). Each chip was the same size, such that both the total fluidic channel area and total area between channels was the same for each chip [64].**

The microfluidic channel arrays were fabricated from PDMS against SU-8 moulds using the process explained in Section 3.2. The PDMS arrays were manually cut into the same size rectangular shapes (approximately 5 cm x 2.5 cm) and placed on the surface of a Petri dish (Figure 4.2). The PDMS channels and the inner and outer surface of the Petri dishes were washed with ethanol and DPBS same as explained in Section 3.2.

Silicone isolators (Grace Bio-Labs) or silicone sealants (Dow Corning) were used to make a same-sized barrier around each microfluidic channel array in order to provide a larger volume of fluid as required by the sensor (0.55 ml for the silicone isolators, or 4.5 ml for the silicone sealant isolators) compared to the volume of only the microfluidic channels in each array (0.009 ml).

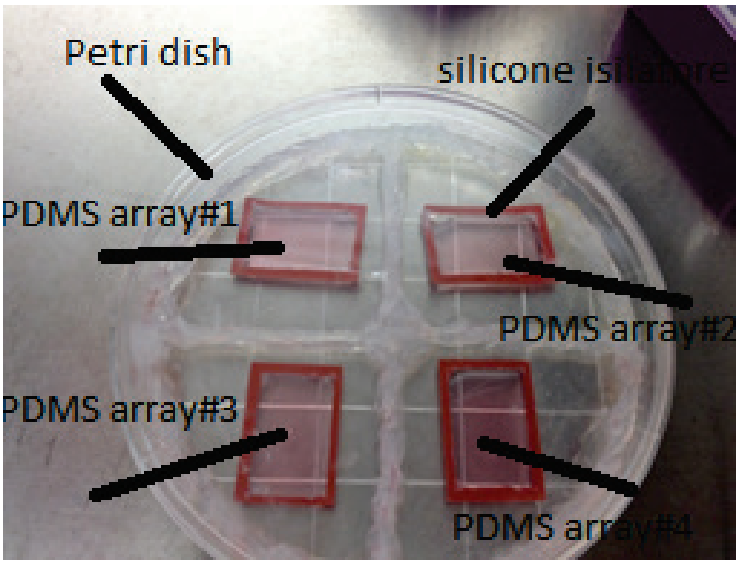

(a)

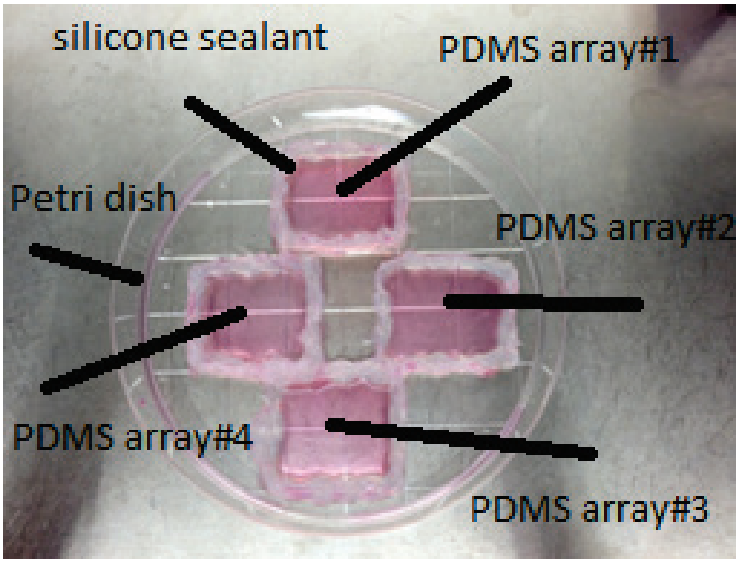

(b)

Figure 4.2 **a) Silicone isolators; and b) silicone sealant isolation used to seal and make barriers around the channel arrays. The cell medium is the pink fluid shown covering each of the four arrays inside the square-shaped isolators. The Petri dish diameters are 150 mm [64].**

4.2. Experimental Methods

Collagen was coated on the surface of each array according to the procedure explained in Section 3-1. The total volume of 12 ml of collagen solution (11800 µl of acetic acid and 200 µl of collagen) was mixed and added to the arrays equally (3 ml each array). BAECs were cultured using the same procedures as for the single microfluidic channel experiment in Section 3.3.

After performing the first few tests, silicone sealants were found to be more convenient in making barriers around the arrays since they increase the possible maximum volume of cell culture medium to 4.5 ml, while silicone isolators increase the volume only up to maximum 0.55 ml. However, in each test only 3 ml of the possible 4.5 ml volume was used. This was done to facilitate manual extraction of 0.5 ml samples for testing from each device. Silicone sealant was used to provide a barrier with the dimensions of approximately 4.5 cm x 2 cm and a depth of 0.5 cm. For the experiment done with different size channel width, seven different chips tested at each of the four different fluidic channel widths.

To ensure that the measurements were performed on approximately the same number of cells (cells grown just inside the channels), the cells cultured on the areas between the channels were scraped 24 hours after cell plating. The scraper's highly compliant thermoplastic elastomer blade pivots to provide multiple angles to remove cells from entire growth surfaces. There is a flexible joint between the blade and handle, which improves ease of access into the corners of the fluid reservoir when it is used to scrape the cells on the surfaces surrounded by the silicone isolators. Figure 4.3 shows the BD Falcon scraper used in these experiments. Moving from one channel to another, the blade part of the scraper had to be washed by rinsing the scraper in a tube of fresh DMEM. This cell-scraping technique step was developed solely for this thesis, and provided a new and easy and effective method of comparing cell populations grown on different chips and in microfluidic channels of different widths.

Figure 4.3 Photograph of a cell scraper from BD Falcon: 18 cm handle and 1.8 cm blade.

Photographs of ECs cultured inside and outside of microfluidic channels before and after cell scraping are shown in Figure 4.4. Figure 4.4a and 4.4b show confluent ECs before (a) and after (b) scraping in the 3 mm-wide fluidic channel. Figure 4.4c shows confluent cells grown inside and outside 100 μm-wide microfluidic channels and Figure 4.4d shows 200 μm-wide microfluidic channels after the cells grown outside the channels have been scraped.

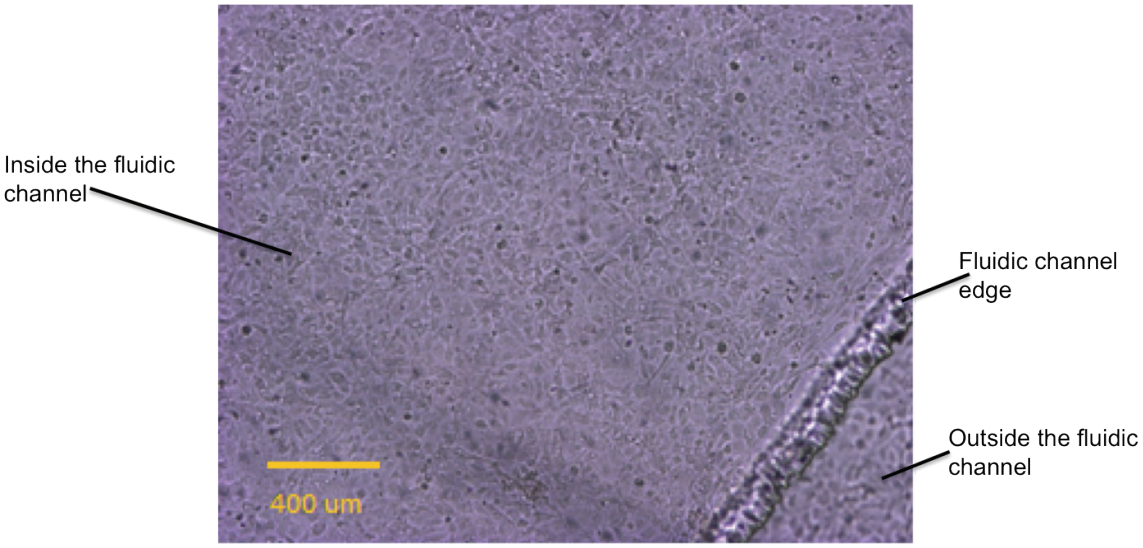
Inside the fluidic channel
Fluidic channel edge
Outside the fluidic channel
400 um

(a)

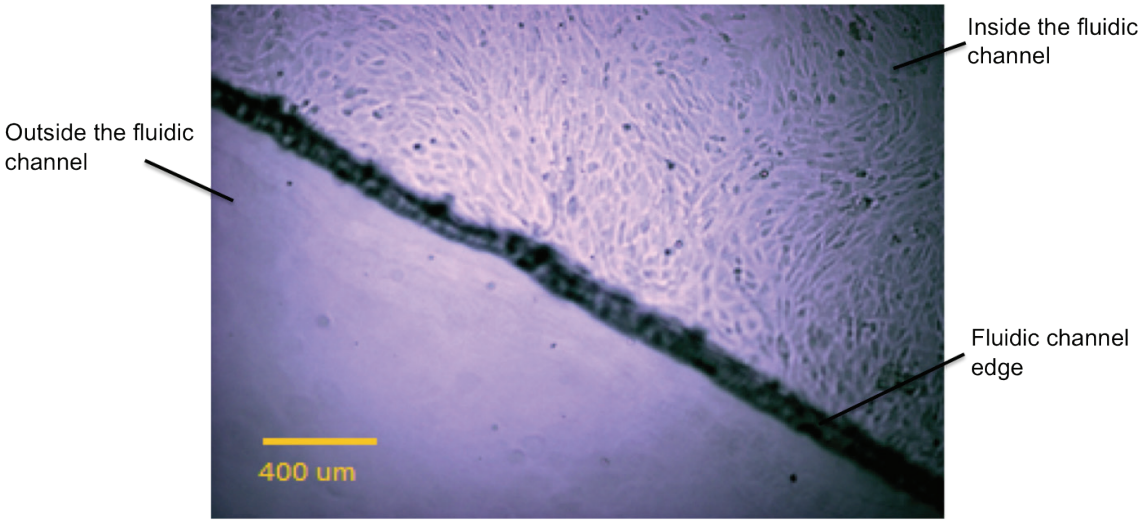
Outside the fluidic channel
Inside the fluidic channel
Fluidic channel edge
400 um

(b)

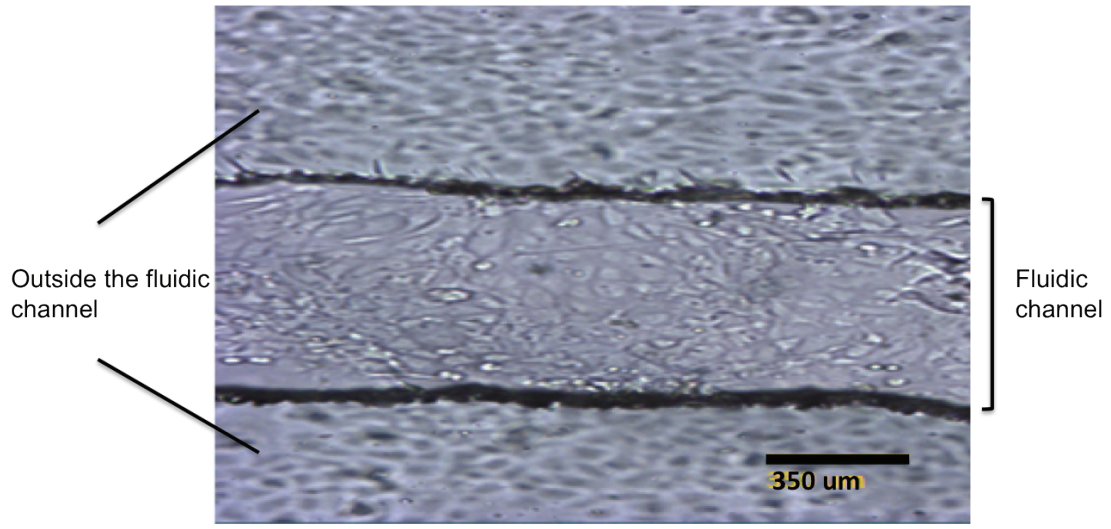

(c)

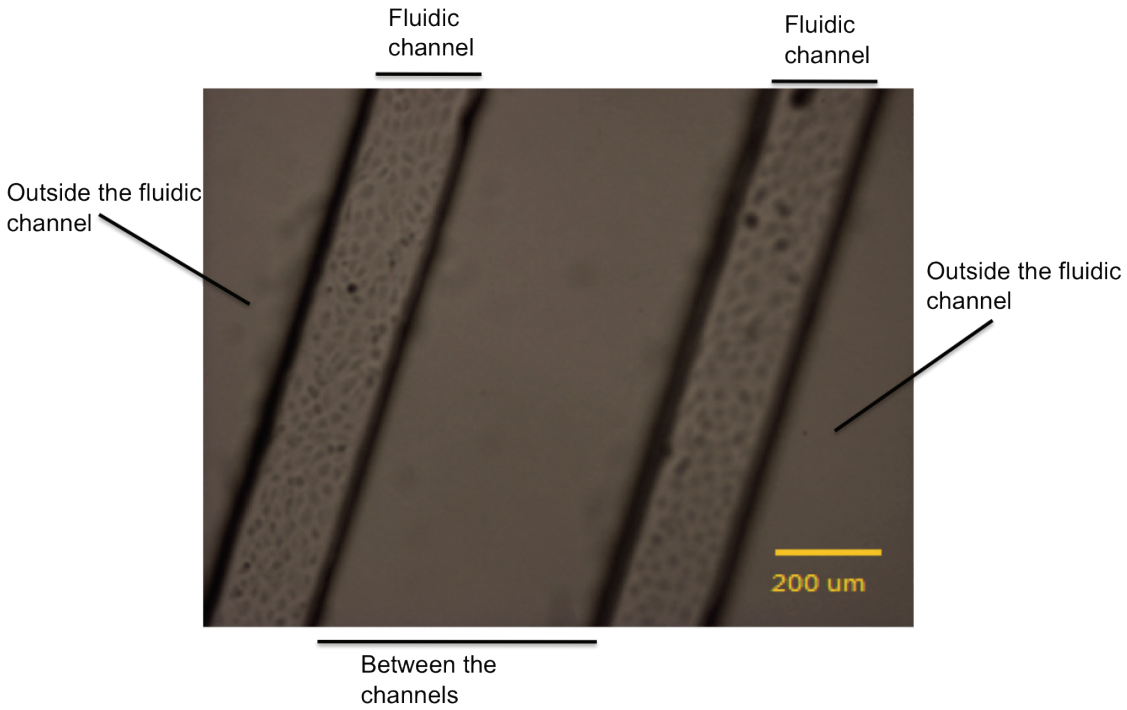

(d)

Figure 4.4 **Photographs of EC monolayers cultured in microfluidic channel arrays: a) inside and top of a fluidic channel before cell scraping; b) inside and top of a fluidic channel after cell scraping; c) between two microfluidic channels before cell scraping; and d) between two microfluidic channels after cell scraping [64]**

The remaining cells were then washed and provided with 3 ml of fresh medium (not filled up to 4.5 ml) in each array, and then left in the incubator for another 24 hours. Approximately 0.5 ml of medium was collected from each microfluidic channel system and centrifuged to remove cellular debris before being stored in at -80 ^{o}C until tested for NO concentration. To obtain the average NO concentration for each fluidic channel width (3 mm, 300 μm, 200 μm, and 100 μm), seven different chips for each fluidic channel width were tested in triplicate. Thus, 28 tests (seven chips each for the four different fluidic channel widths) were performed in triplicate to minimize errors.

An ozone-chemiluminescence-based sensor system (NOA 280i, Sievers Nitric Oxide Analyzer) was utilized to detect and measure the amount of NO in the samples as explained in Section 3.4. Using this sensor we developed a simple protocol for measurements from microfluidic structures. The NO released from the ECs cultured in different channel sizes (resulting in differently-shaped ECs) could thus be detected.

4.3. Experimental Results

The concentration of NO released from cell monolayers cultured within microfluidic channels of different widths was measured and compared. Table 4.2 shows the mean value of NO concentration among the seven samples for each microfluidic channel width from seven different chips, along with one standard deviation and standard error for each data set at each microfluidic channel width. The standard error for each data set was calculated by dividing the standard deviation by the square root of the number of samples (7 samples). There was a time interval of at least a week between testing each of the seven samples so every time a new standard curve was generated and the calculations were done due to the standard curve.

Table 4.2 **The results of each seven samples, mean value, standard deviation, and standard error calculated for each data set at each microfluidic channel width; Array#4, Array#3, Array#2, and Array#1 are the arrays with 1, 10, 15 and 30 microfluidic channels respectively as introduced in Table 2. The unit for all values is nM.**

	Array#4: 1 3-mm channel	Array#3: 10 300-μm channels	Array#2: 15 200-μm channels	Array#1: 30 100-μm channels
Sample 1	1631.36	1685.62	1453.01	1919.41
Sample 2	1541.41	1340.18	1493.59	1497.82
Sample 3	1706.44	1540.22	1329.14	1395.35
Sample 4	1438.98	1547.13	1696.30	1402.26
Sample 5	1420.86	1480.19	1388.07	1395.62
Sample 6	1518.88	1523.12	1431.36	1430.44
Sample 7	1240.67	1291.52	1379.59	1459.55
Mean	1499.80	1486.85	1453.01	1500.07
Standard Deviation	152.30	133.55	131.34	188.75
Standard Error	57.56	50.47	53.62	71.34

It has been previously mentioned that the degree of elongation of BAECs increases as microfluidic channel width decreases. A similar microfluidic channel width-dependence for EC elongation has been seen for BAECs grown in the microfluidic system presented in this thesis. However, our simple and versatile microfluidic culture and NO-measurement system also enabled us to measure the NO release of cells grown in microfluidic channels of different sizes. Figure 4.5 shows the NO concentration as a function of microfluidic channel width (which correlates to different degrees of cell elongation). To determine if there was statistically significant difference between different groups, Analysis of Variance (ANOVA) test [67,68] was performed using the data in Table 4.2. It was shown that there was no statistically significant differences between group means as determined by ANOVA ($F(3,24)$=0.1510, p=0.9280). So these first results suggested that there was no statistically significant change in the amount of NO released from cells in different microfluidic channel sizes. Thus, it appears that physically forcing the cells in microfluidic channels to become less or more elongated may not significantly affect the generation of NO. This compares to results for shear-stress

elongated cells in which NO production increases for more elongated cells due to application of sufficient shear stress [53]; however, more experimentation is needed to verify the seeming lack of difference between NO production in microfluidic and fluidic channels of difference sizes as indicated by our first results here.

It is noted that for the first 24 hours of this experiment, the cells had also plated between the channels, which would be expected to lead to the same level of NO measurement among all samples. However, even after another 24 hours of NO release only by cells in the fluidic channels, a difference was still not discernable as shown in Table 4.2 and Figure 4.5. Although further testing is needed to determine if these results are indeed representative, the results show successful proof-of-concept for the devices and methodologies developed in this thesis, and the ability to measure NO concentration in many different samples from cells cultured in microfluidic channels of different widths. This is also indicated from the graph, in that there are very large standard deviation bars compared to the mean values and that all mean values fall within each others' error bars.

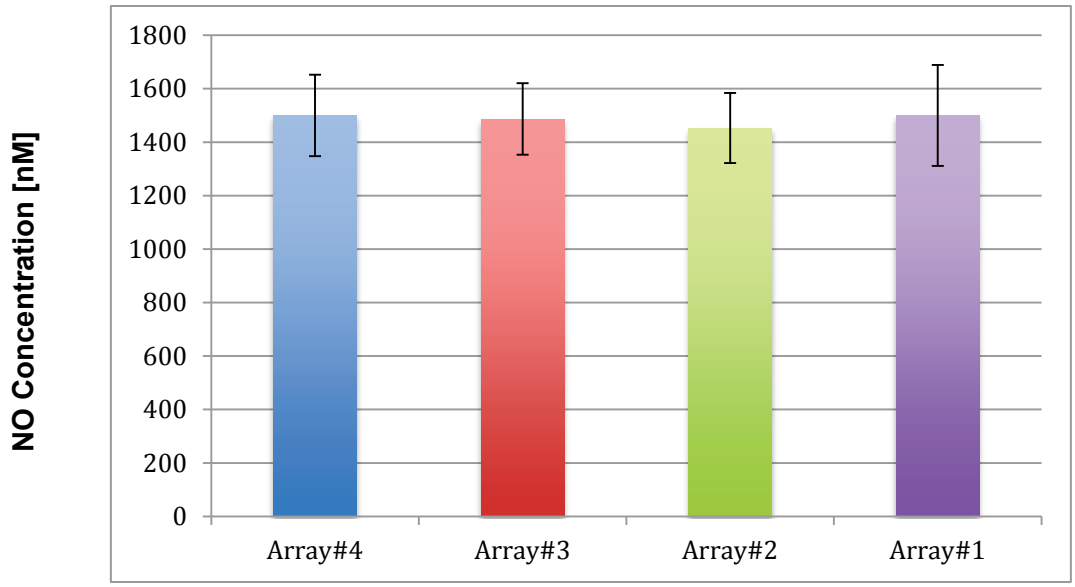

Figure 4.5 **The graph of mean value of NO concentration released from the cells cultured within microfluidic channels of different widths. Array#4 is the array with 1 3-mm channel and Array# 3, Array#2 and Array#1 are the arrays with 10 300-μm, 15 200-μm, and 30 100-μm microfluidic channels, respectively, as introduced in Table 2 [64]. The error bars each shows one standard deviation for that data set.**

Chapter 5.

TNFα-stimulated Endothelial Cells

TNFα is a pro-inflammatory cytokine (cell signalling protein), which has been shown to increase both EC elongation and acute NO secretion [69,70]. It has been previously shown in a study that the amount of NO released into the medium conditioned by untreated and TNFα treated ECs cultured in 35 mm culture dishes was 1.81± 0.17 μM and 2.86 ± 0.29 μM respectively and so stimulation of ECs with TNF-α increased NO release 58% [70]. In this chapter, it is investigated whether or not the stimulatory effect of TNFα on ECs cultured within the microfluidic channel-based system was significant. The purpose of this experiment was to investigate the versatility of the system, i.e., to show that multiple stimulants (e.g., microfluidic channel confinement and chemical stimulation) could be acted on the cells simultaneously. Furthermore, the experiments were performed in order to determine if the influence of cytokines on ECs could be studied in the microfluidic system as previously studied in traditional culturing systems. For this purpose array#4 (3 mm-wide fluidic channel) and array#1 (100 μm-wide microfluidic channels) from Section 4.1 were chosen for this experiment.

5.1. Experimental Methods

The PDMS channels against SU-8 moulds were fabricated using the same process as outlined in Section 3.2. ECs were plated on the surface of two identical arrays of each size, and cultured using the same basic procedures described previously in Section 4.2. However, there were a few alterations: the cells grown outside of the fluidic channels were scraped at the 6 hour time point in this experiment. The ECs were then washed and provided with fresh media. One of the fluidic channels was then treated with 10 μl/ml of TNFα using a micropipette. To get better results, the TNFα and

fresh media was first mixed using a vortex mixer and then the solution was added to each channel instead of filling the channels with fresh media and then adding TNFα.

Both the treated and non-treated cells were incubated for another 18 hours. Two 0.5 ml samples were then collected after this time period, one each from the treated and non-treated fluidic channel devices. Thus, the total time for this process was 24 hours less than the two previous processes; therefore it is expected that the cells would release less NO than the other two experiments as the time period for release was less than half as long.

5.2. Experimental Results

TNFα increases the elongation and acute NO generation of ECs in conventional culturing dishes. In this experiment, the influence of TNFα on the shape and function of ECs cultured in fluidic channels was investigated in order to show the versatility of the system to easily perform such experimentation. The quantity of NO released from treated and untreated ECs cultured within two identical fluidic channels was measured and compared in this experiment. The results showed that TNFα increased NO production. In addition, the previously un-elongated cells (as expected in a fluidic channel 3-mm in width) became elongated in the fluidic channel due to TNFα stimulation. This experiment was repeated five times on samples obtained from the same chips under the same conditions for 3-mm-wide fluidic channels and four times for 100 μm-wide microfluidic channels. The average value of the results from all five experiments for 3 mm-wide fluidic channels and four experiments for 100 μm-wide microfluidic channels were calculated.

Figures 5.1a and 5.1b show pictures of untreated ECs and TNFα-treated ECs (cultured in 3 mm-wide fluidic channel) approximately 18 hours after scraping and adding the TNFα (which occurred at the 6 hour time point). As can be seen in Figure 17b, not all of the treated cells appear to be elongated, but there are many elongated cells compared to mainly cuboidal cells in the untreated sample. However, there were not many elongated cells observed in the 100-μm-wide microfluidic channels after treating the cells with TNFα compared to the number of treated cells in the 3 mm-wide

fluidic channel. This may be due to existing cytoskeletal rearrangement on the cells cultured in the relatively thin microfluidic channel [12].

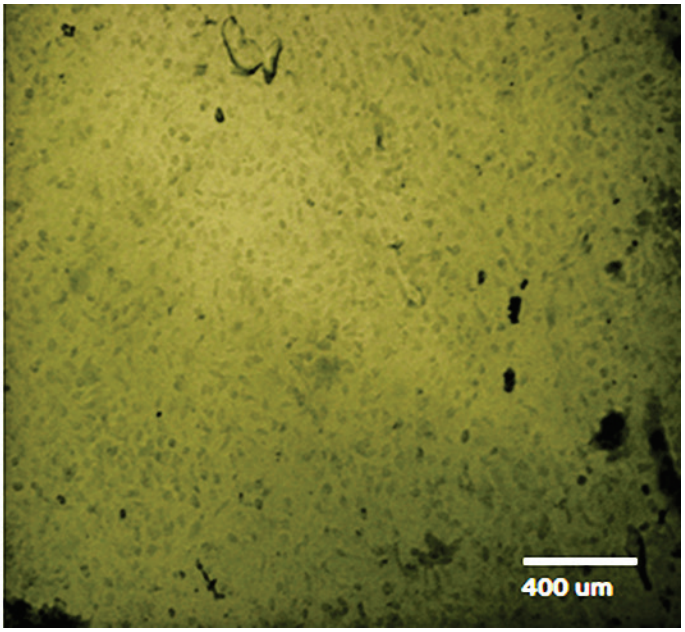

(a)

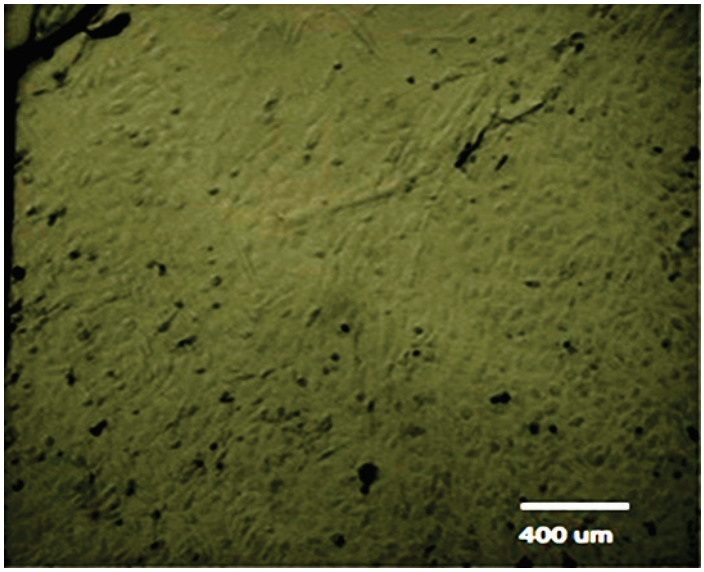

(b)

Figure 5.1 Endothelial cells 18 hours after being scraped (24 hours after plating): a) untreated; and b) treated with TNFα at the 6 hour time point. These figures show cells in a 3-mm-wide channel [64].

Table 5.1 and Table 5.2 provide the results of NO concentration released from TNFα-treated and untreated ECs cultured in 3 mm-wide fluidic channels in five experiments and 100-μm-wide microfluidic channels in four experiments, respectively. The mean value of the results, standard deviation, and standard error are also shown in Table 5.1 and Table 5.2. Figure 5.2 and Figure 5.3 also show the average value of NO concentration released from the TNFα-treated and untreated endothelial cells cultured in 3 mm-wide fluidic channels and 100 μm-wide microfluidic channels.

Table 5.1 The results of five samples, mean value, standard deviation and standard error of NO concentration released from cells cultured in two identical 3-mm-wide fluidic channels. The cells in one channel were treated with TNFα . The unit for all values is nM.

	Non-treated ECs	Treated ECs
Sample 1	208.56	249.04
Sample 2	287.58	294.76
Sample 3	123.25	200.55
Sample 4	179.01	226.50
Sample 5	96.66	161.66
Mean	179.01	226.50
Standard Deviation	75.08	50.11
Standard Error	33.57	18.66

Table 5.2 The results of five samples, mean value, standard deviation and standard error of NO concentration released from cells cultured in two identical 100-μm-wide microfluidic channels. The cells in one channel were treated with TNFα . The unit for all values is nM.

	Non-treated ECs	Treated ECs
Sample 1	276.32	302.01
Sample 2	283.85	297.38
Sample 3	321.59	328.3
Sample 4	343	350.37
Mean	306.19	319.51
Standard Deviation	31.53	24.66
Standard Error	15.76	12.33

The difference between the treated and non-treated NO production was thus 26.52% and 4.35% for the 3-mm-wide channel and the 100 μm-wide microfluidic channel, respectively. Thus, while there was an increase, as would be expected based on previous results from cells grown in petri dishes [70], the amount was not as great, especially in the case of the microfluidic channel. To determine if there was a statistically significant difference between treated and untreated groups in both 3 mm-wide fluidic channels and 100 μm-wide microfluidic channels, an ANOVA test was performed using the data in Table 5.1 and Table 5.2. It was shown that there was no statistically significant differences between group means in both 3 mm-wide fluidic channels and 100 μm-wide microfluidic channels as determined by ANOVA ($F(1,8)$=1.3836, p=0.6218 and $F(1,6)$=0.4430, p=0.8502 for 3 mm-wide fluidic channels and 100 μm-wide microfluidic channels respectively) and so the difference between NO production from treated and non-treated ECs cultured in both fluidic channel sizes was not significant according to this initial study. This is also indicated from the graph, in that there are very large standard deviation bars compared to the mean values and that both mean values fall within the others' error bar. However, further experimentation may yield different results. It is interesting to note that the 100 μm-wide microfluidic channel yielded almost no difference in NO production between treated and untreated monolayers. As these are the first known results discussing the NO production of ECs in microfluidic channels with TNFα stimulation, further experimentation is required to verify these results.

The stimulatory effect of TNFα on ECs cultured within the microfluidic channel-based system was investigated in this Chapter. It was shown that multiple stimulants (e.g., microfluidic channel confinement and chemical stimulation) could be acted on the cells simultaneously. However it was determined that the influence of TNFα on ECs was not significant compared to results obtained in a Petri dish according to the ANOVA test; even though the results were as expected (NO concentration higher for treated cells), these first results were not statistically significant.

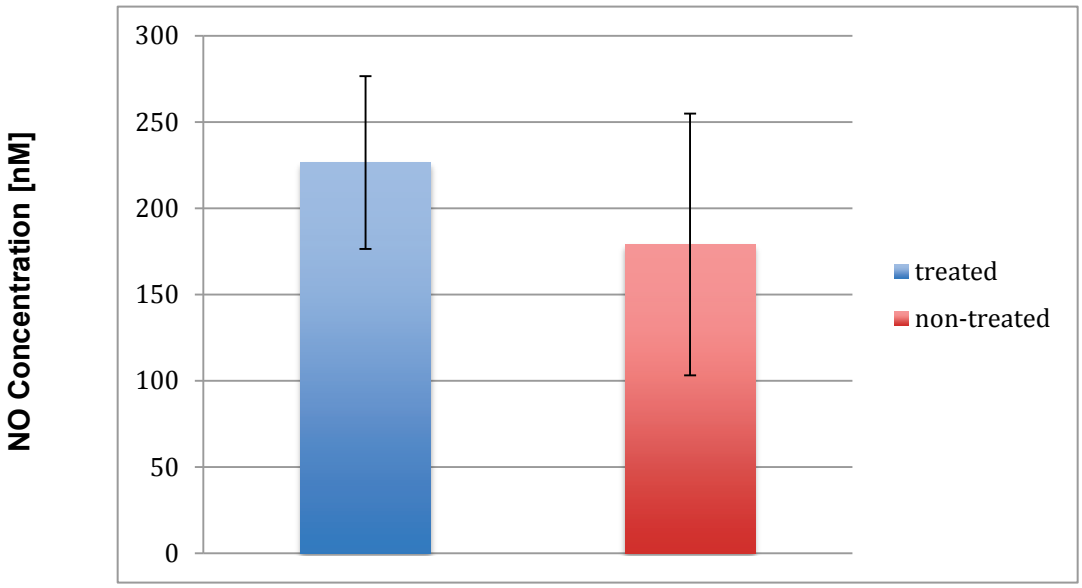

Figure 5.2 **Mean value of NO concentration released from cells cultured in two identical 3-mm-wide fluidic channels. The cells in one channel were treated with TNFα. The standard error for the data sets was 18.66 and 33.57 for treated and untreated ones, respectively [64]. The error bars each shows one standard deviation for that data set.**

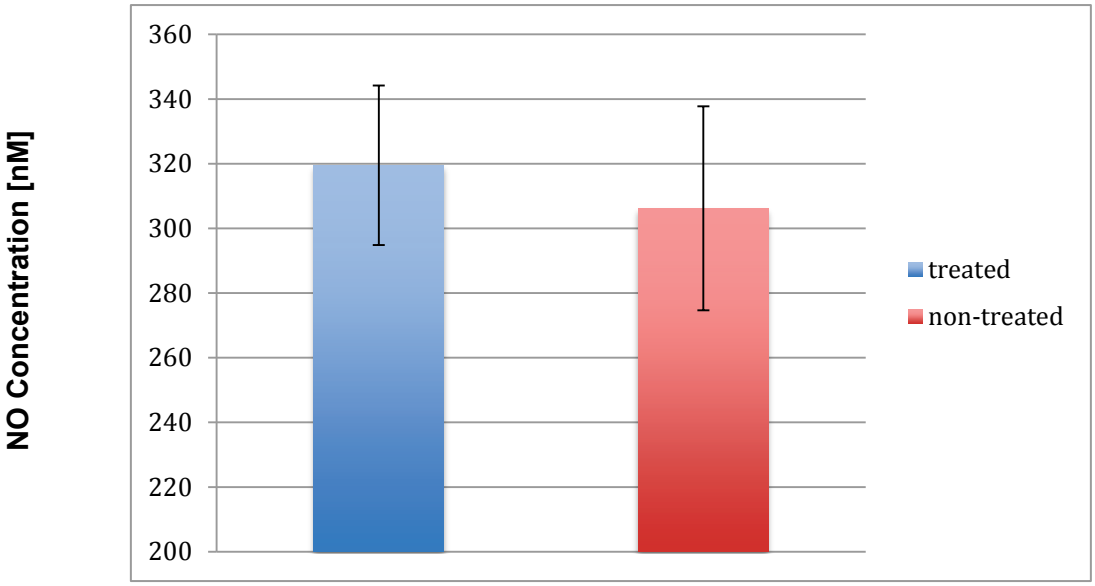

Figure 5.3 **Mean value of NO concentration released from cells cultured in two identical 100-μm-wide microfluidic channels. The cells in one channel were treated with TNFα. The standard error for the data sets was 12.33 and 15.76 for treated and untreated ones, respectively. The error bars each shows one standard deviation for that data set.**

Chapter 6.

Future Work

In this thesis, a microfluidic system is developed and tested to prove its capability and to show proof-of-concept, but the device and method are not optimized. Although the system provides the capability for a range of morphological and functional studies, optimization is needed to enhance the design for a flow through system with thinner microfluidic channels that are closer to EC cell size, which would result in more significant microfluidic channel-induced elongation. Furthermore, it is possible that the non-significance of the ANOVA test for the TNF-α samples is due to error introduced by the manual methods performed in this thesis and improved and more uniform fabrication of the isolators and more controlled or automated sample volume transfer techniques to the sensor, may improve errors and result in improved results. A larger number of samples may also improve results; however, a large number of measurments would require access to an NO sensor exceedingly that available for the exploratory research presented in this thesis. Please see Chapter 7 for a more thorough discussion.

A preliminary work has been done to optimize the previous design to a flow through system to be used in future with cells, which is briefly described in this chapter. While minimizing the size of microfluidic channels in a system, which enables the control the cell shape with flow or without flow, it is important to maintain the same culturing surface area (same number of cells). In order to maintain the cell culturing area, a system is designed which consists of micro-patterned silicone chambers and microfluidic channels of different geometries. The samples are designed to have the same culturing surface area for each microfluidic channel, with different channel length for each different width of channel (thinner channels are longer). The microfluidic flow system consists of 5 microfluidic channels with the same depth but varying widths from 40 μm to 220 μm and varying length from 1000 μm to 5500 μm in order to provide the same

surface area for each channel. Table 6.1 shows the dimensions of each microfluidic channel, which are numbered 1 through 5.

Table 6.1 Dimensions for different flow-through microfluidic channels

Microfluidic channel #	Width (μm)	Length (μm)	Depth (μm)
1	40	5500	100
2	80	2750	100
3	120	1833.33	100
4	160	1375	100
5	220	1000	100

The same fabrication process as presented in this thesis is used for microfluidic chips for no-flow conditions. However, in this design, an additional step is added, which is bonding of a PDMS lid, using oxygen plasma, for sealing of the channels (see Figure 6.1). Figure 6.2 shows a close-up photograph of the fabricated SU-8 mould. Figure 6.3 shows an example completed device with enclosed microfluidic channels and tubing for inlet/outlet of fluid samples.

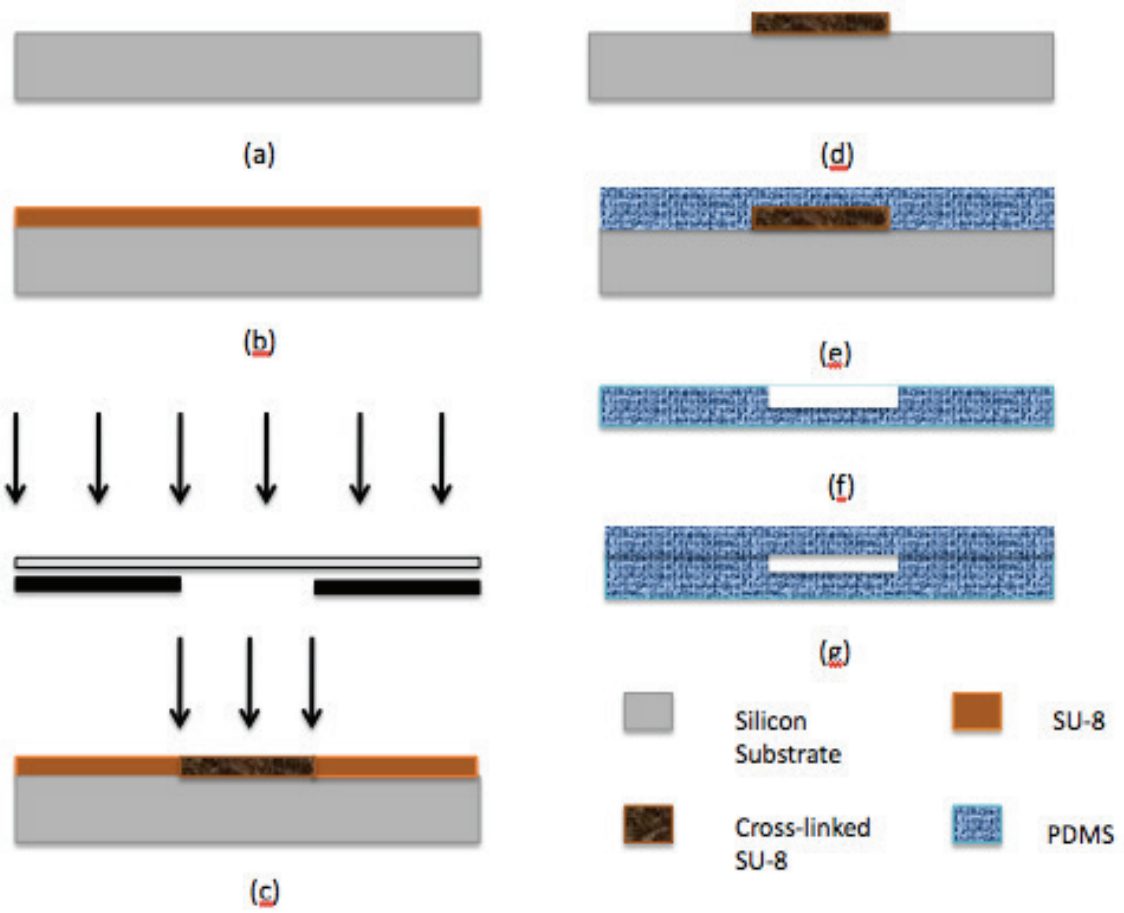

Figure 6.1 **Fabrication process for 100-µm thick SU-8 mould and PDMS microfluidic channels: a) clean the wafers with an RCA 1 clean; b) spin SU-8 photoresist and pre-bake; c) expose and post-exposure bake; d) develop e) pour liquid PDMS (10:1 mass ratio of base and curing agent, Dow Corning); f) peel PDMS layer; g) bonding of PDMS lid to the channels and formation of access holes for tubing**

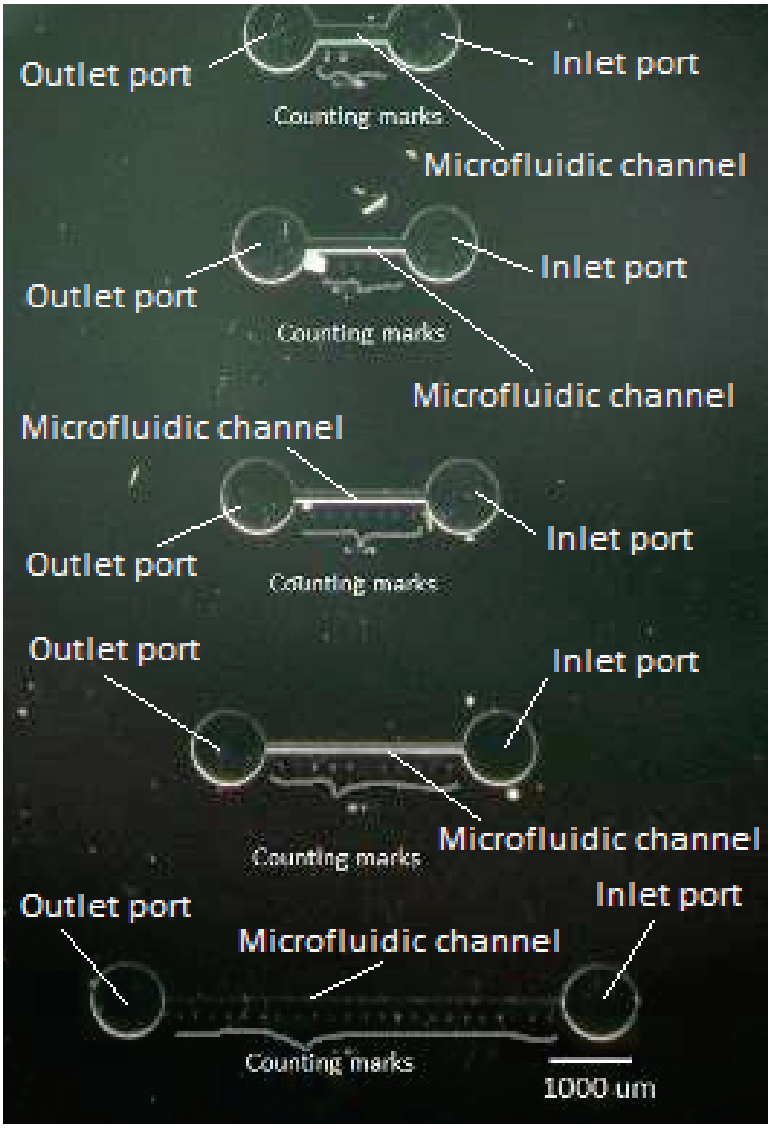

Figure 6.2 Photograph of the SU-8 mould

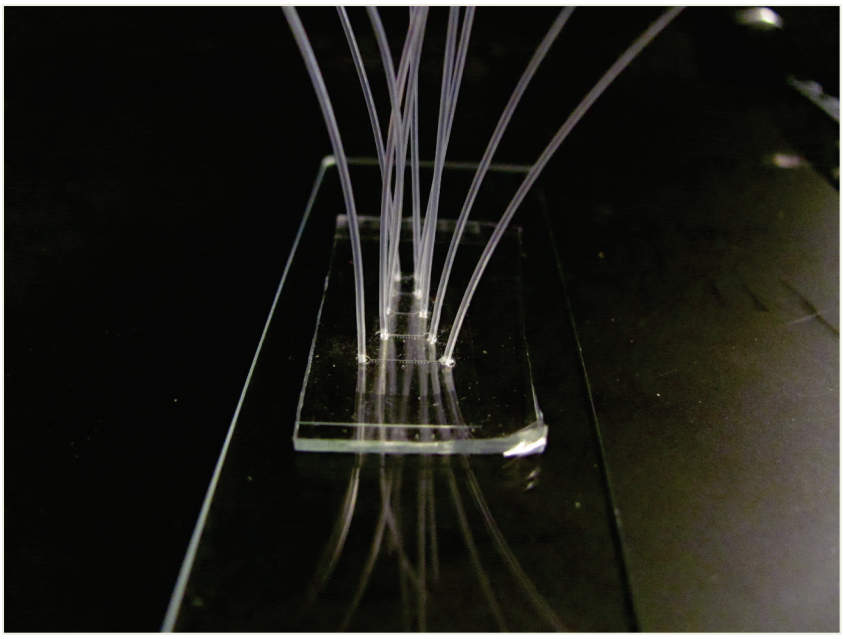

Figure 6.3 The integration of microfluidic channels with inlet and outlet tubing for flow testing

In the future this work will be completed and the flow through system will be fabricated and so ECs will be cultured within the microfluidic channels of varying widths and varying length to study the influence of multiple stimulants (e.g., microfluidic channel confinement and shear stress), which will provide more capability for ECs morphological and functional studies.

Other future work will involve to determine the influence of TNFα or some other drugs on NO production by ECs cultured within microfluidic channels of this optimised design (different widths and length but same culturing surface). The effects of different chemical stimuli rather than TNFα will be also studied on ECs elongation and NO production under flow and without flow.

Chapter 7.

Discussion and Conclusions

A simple microfluidic system and NO detection method has been developed that enables simultaneous study of the effects of EC shape control and chemical stimuli on NO production by ECs in microfluidic structures. A highly versatile system is designed that does not have an integrated NO sensor, thus avoiding (such sensor's difficulties of design, fabrication, calibration, and drift. Instead, the method developed in this thesis uses state-of-the-art NO measurement equipment, and provides the necessary capabilities for a range of EC morphological and functional studies.

The microfluidic culturing system consists of four arrays of PDMS microfluidic channels of the same length and depth, but varying widths. The microfluidic channels were fabricated using standard soft lithography. In order to have a similar number of cells in each array, the arrays were designed to have the same culturing surface area (75 mm^2) regardless of fluidic channel width, i.e., a greater number (30) of thinner (100 μm-wide) microfluidic channels were used compared to a fewer number (1) of wider (3 mm-wide) fluidic channels in order to obtain the same culturing surface area. A cell scraping process was developed in order to remove cells between fluidic channels after confluence so that only cells cultured within the confines of the fluidic channels would contribute to NO production in the later hours of the experiment (after scraping).

Initial results show that NO can indeed be measured in the microfluidic channel systems using the newly developed methods. The mean value for the NO concentration from the cells cultured in 100 μm-wide, 200 μm-wide, and 300 μm-wide microfluidic channels, and 3 mm fluidic channel was 1500.07±71.344 nM, 1453.013±53.621 nM, 1486.859±50.477 nM, and 1499.805±57.566 nM, respectively. These results may suggest that physically changing the morphology of the ECs does not affect NO

production, although further study is necessary to confirm these results. It is noted that for the first 24 hours of this experiment, the cells had also plated between the channels, which would be expected to lead to the same level of NO measurement. Thus, the experiment could be improved with earlier cell scraping provided all cells were first allowed to plate out of solution. Another potential source of error is that some cells remain on top of the channels after scraping, although the number of remaining cells is very small and thorough scraping is ensured via microscopic examination. Other potential sources of error include differences in the amount of fluid volume containing suspended cells and amount of cell medium added (0.55 ml or 3 ml depending on test); these steps are all currently performed manually using a pipette. While ensuring versatility and simplicity for the measurement method, these manual steps no doubt introduce error into the amount of fluid dilution and, thus, NO concentration. A more automated procedure should result in less variability. In addition, the silicone sealant barriers are currently fabricated by hand; thus, the area of cell culture surface not contained within fluidic channels may vary slightly from chip to chip. While using a relatively large number of different chips with different barriers (e.g., the seven chips used for the baseline measurements) minimizes this problem, it is at the expense of more time consuming tests.

Cells were also stimulated with the pro-inflammatory cytokine TNFα in order to investigate the versatility of the instrument for performing different tests that may result in altered NO production by ECs grown in fluidic channels. The resulting NO concentrations (226.50615±18.6691 nM vs. 179.0183±33.5786 nM for treated and untreated cells respectively) in 3 mm-wide fluidic channel) and (306.1942±15.7869 nM vs. 319.5182±12.3335 nM for treated and untreated cells respectively) in 100 μm-wide microfluidic channels) suggested that the stimulated ECs became more elongated and released more NO than cells not stimulated with the cytokine, which was an expected result based on data from conventional culturing dishes; however, the ANOVA test indicates that this difference is not statistically significant for both microfluidic channels or fluidic channels. Although the difference between the NO produced by the untreated and TNFα-treated samples was approximately 20%, it is still somewhat lower than what is seen in other experiments in culturing dishes. However, this experiment was based on results from a single fluidic chip; thus, more experimentation is needed to further validate

these results. As the time period for NO release in this process was 24 hours less than the two previous processes, the absolute value of the amount of NO detected was less compared to the single channel and baseline measurements at each microfluidic channel width.

Other future work will involve performing the same experiment on microfluidic channels of different widths to determine the effect of TNFα on the NO production of already elongated ECs in microfluidic channels. Such experimentation will show not only further versatility of the microfluidic system and method for NO measurement developed and demonstrated as proof-of-concept in this thesis, but will herald the beginning of experiments that may have significant biological relevance to vascular research.

References

[1] P. Tabeling, Introduction to microfluidics, oxford university press, 310(2005)

[2] N. Nam-Tung, and T.W. Steven, Fundamentals and applications of microfluidics, 471(2002)

[3] V.V. Abhyankar, A.L. Lokuta, A. Huttenlocher, D.J. Beebe, “Characterization of a membrane-based gradient generator for use in cell-signaling studies “ *Lab on a chip*, Vol. 6, pp. 389-393, 2006

[4] B.G. Chung, L.A. Flanagan, S.W. Rhee, A.P. Lee, E.S. Monuki, N.L. Jeon, “Human neural stem cell growth and differentiation in a gradient-generating microfluidic device” *Lab chip*, Vol. 5, no.1, pp. 401-406, 2005

[5] D. Irimia, S.Y. Liu, W.G. Tharp, A. Samandari, M. Toner, M.C. Poznansky, “Microfluidic system for measuring neutrophil migratory responses to fast switches of chemical gradients” *Lab chip*, Vol. 6, no. 2, pp. 191-198, 2005

[6] A.D. Van der meer, A.A. Poot, M.H.G. Duits, J. Feijen, and I. Vermes, “Microfluidic technology in vascular research”, J*ournal of Biomedicine and Biotechnology*, Vol. 2009,10 pages, 2009

[7] F. Bedioui, D. Quinton, S. Griveau, and T. Nyokong, “Designing molecular materials and strategies for the electrochemical detection of nitric oxide, superoxide and peroxynitrite in biological systems” *Physical Chemistry Chemical Physics*” Vol. 12, pp. 9976-9988, 2010

[8] D.B. Cines,E.S. Pollak, C.A. Buck, J. Loscalzo, G.A.R.P. McEver, J.S. Pober, T.M. Wick, B.A. Konkle, B.S. Schwartz, E.S. Barnathan, K.R. McCrae, B.A. Hug, A. Schmidt, and D.M. Stern, “Endothelial Cells in Physiology and in the Pathophysiology of Vascular Disorders” *The Journal of The American Society of Hamatology*, Vol. 91, pp. 3527-3561, 1998

[9] S. Letourneae, L. Hernandez, A.N. Faris, D.M. Spence, “Evaluating the effects of estradiol on endothelial nitric oxide stimulated by erythrocyte-derived ATP using a microfluidic approach”, *Analytical and Bioanalytical Chemistry*, Vol. 397 no. 8, pp. 3369-3375, 2010

[10] C. Claudio Napoli, and L. Ignarro, “Nitric Oxide and Atherosclerosis”, *Elsevier*, Vol. 5, no. 2, pp. 88–97, 2001

[11] A.L. Barakat, and D.K. Lieu, "Differential responsiveness of vascular endothelial cells to different types of fluid mechanical shear stress", *Cell Biochemistry and Biophysics*, Vol. 38, pp. 323-343, 2003

[12] B.L. Gray, D.K. Lieu, S.D. Collins, R.L. Smithe, and A.I Barakat, "Microchannel platform for the study of Endothelial cell shape and function", *Biomedical microdevices*, Vol. 4, no. 1, pp. 9-16, 2002

[13] M.D. Flame, I.H. Sarelius, "Flow-induced cytoskeletal changes in endothelial cells growing on curved surfaces", *Microcirculation*, Vol. 7, no. 6, pp. 419-427, 2000

[14] K. Liu, R. Pitchimani, D. Dang, K. Bayer, T. Harrington, D. Pappas, " Cell culture chip using low-shear mass transport", *Langmuir*, Vol. 24, no. 11, pp. 5955-5960, 2008

[15] C.F. Dewey, S.R. Bussolari, M.A. Gimbrone, and P.F.Davies, "The dynamic response of vascular endothelial cells to fluid shear stress", *Journal of Biomechanical Engineering*, Vol. 103, no. 3, pp. 177-185, 1981

[16] R.M. Nerem, M.J. Levesque, and J.F. Cornhill, "Vascular endothelial morphology as an indicator of the pattern of blood flow", *Journal of Biomechanical Engineering*, Vol. 103, no. 3, pp. 172-176, 1981

[17] C.S. Chen, M. Mrksich, S. Huang, G.M. Whitesides, and D.E. Ingber, "Geometric control of cell and death" *Science*, Vol. 276, no. 5317, pp. 1425-8, 1997

[18] R. Singhvi, A. Kumar, G.P. Lopez, G.N. Stephanopoulos, D.I.C. Wang,G.M. Whitesides, and D.E. Ingber, "Engineering cell shape and function" *Science* Vol. 264, no. 5159, pp. 696-698, 1994

[19] B.J. Spargo, M.A. Testoff, T.B. Nielsen, D.A. Stenger, J.J. Hickman, and A.S. Rudolf, "Spatially controlled adhesion, spresding, and differentiation of endothelial cells on self-assembled molecular monolayers" *Proceedings of the National Academy of Sciences*,*USA*, Vol. 91, no. 23, pp. 11070-11074, 1994

[20] A. Shamloo, N. Ma, M. Poo, L. Sohn, S. Heilston, "Endothelial cell polarization and chemotaxis in a microfluidic device", *Lab on a chip*, issue 8, pp. 292-1299, 2008

[21] G.A. Dunn and A.F. Brown, "Alignment of fibroblasts on grooved surfaces described by a simple geometric transformation", *Journal of Cell Science*, Vol. 83, no. 1 pp. 313-340, 1986

[22] C. Oakley and D.M. Brunette, "The sequence of alignment of microtubulus, focal contacts and actin filaments in fibroblasts spreading on smooth and grooved titanium substrata" *Journal of Cell Science*, Vol.106, no. 1 343-354, 1993

[23] B. Bussolati, C. Dunk, M. Grohman, D. Kontos, J. Mason, A. Ahmed," Vascular endothelial growth factor receptor-1 modulates vascular endothelial growth factor-mediated angiogenesis via nitric oxide" *Am J Pathol*, Vol. 159, no. 3, pp. 993-1008 , 2001

[24] W. Tworetzky, P. Moore, J. Bekker, S.M. Black, J.R. Fineman, "Pulmonary blood flow alters nitric oxide production in patients undergoing device closure of atrial septal defects", *J Am Coll Cardiol*, Vol. 35, no. 2, pp. 463-467, 2000

[25] S. J. George and J. Johnson, "Atherosclerosis: Molecular and Cellular Mechanisms", *Wiley-VCH Verlag GmbH & Co*, 2010

[26] Statistics Canada. (2011c, October). Mortality, summary list of causes 2008. http://www5.statcan.gc.ca/access_acces/archive.action?loc=/pub/84f0209x/84f0209x2008000-eng.pdf&archive=1

[27] WC Aird , "Phenotypic heterogeneity of the endothelium: I. Structure, function and mechanisms", *Circulation Research*, Vol.100, no. 2, pp. 158–173, 2007

[28] M. Félétou", The Endothelium: Part 1: Multiple Functions of the Endothelial Cells—Focus on Endothelium-Derived Vasoactive Mediators", Morgan and Claypool Life Sciences, 2011

[29] PF. Davis, MA. Reidy, TB. Goode, DE. Bowyer "Scanning electron microscopy in the evaluation of endothelial integrity of the fatty lesion in atherosclerosis", *Atherosclerosis*, Vol. 25, no. 1, pp. 125-130, 1976

[30] JT Flaherty, JE Pierce, VJ Ferrans, DJ Patel, WK Tucker, DL Fry, "Endothelial nuclear patterns in the canine arterial tree with particular refernce to hemodynamic events. *Circulation Research*, Vol. 30, pp. 23-33, 1972

[31] SG. Eskin, CL. Ives, LV. McIntire, LT. Navarro "Response of cultured endothelial cells to steady flow", *Microvascular research*, Vol. 28, no. 1, pp. 87-93, 1948

[32] MJ. Levesque, RM. Nerem, "The study of rheological effects on vascular endothelial cells in culture", *Biorheology*, Vol. 26, no. 2, pp. 345-357, 1989

[33] N. Remuzzi, CF. Dewey, PF. Davies, MA. Gimbrone MA. "Orientation of endothelial cells in shear fields in vitro" *Biorheology* , Vol. 21, no. 4, pp. 617-630,1984

[34] Jaffer, S.,Westwood, S., M. and Gray, B. L., "Enclosed SU-8 and PDMS Microchannels with Integrated Interconnect and World-to-chip strucutures," MicroMech.Microeng. 18, 9pges (2008)

[35] GM. Rubanyi, PM. Vanhoutte, "Superoxide anions and hyperoxia inactivate endothelium-derived relaxing factor" *Am J Physiol*, Vol. 250, no. 5 pt 2, pp. H222–7, 1986.

[36] GM. Rubanyi,PM. Vanhoutte, “Oxygen-derived free radicals, endothelium, and responsiveness of vascular smooth muscle”, *Am J Physiol*, Vol. 250, no. 5 pt 2, pp. H815–21, 1986

[37] RJ. Gryglewski, RM. Palmer, S. Moncada, “Superoxide anion is involved in the breakdown of endothelium-derived vascular relaxing factor” *Nature*. Vol. 320, no. 6061, pp. 454–6, 1986

[38] DL. Fry, ”Acute vascular endothelial changes associated with increased blood velocitygradients”, *Circulation research*, Vol. 22, no. 2, pp.165-197, 1968

[39] EW. Young, CA Simmons, “Review Macro- and microscale fluid flow systems for endothelial cell biology”, *Lab chip*, Vol. 10, no. 2, pp. 143-60, 2010

[40] S. Westwood, A. Gojova, B. Kuo, A. I. Barakat, B.L. Gray, “Initial investigation of SU-8 photopolymer as a material for non-invasive endothelial cell research platforms”, *Proc. Of SPIE*, Vol. 6465 64650S-1, 2007

[41] D. Qin, Y. Xia, GM. Whitesides, “Soft lithography for macro- and nanoscale patterning”, *Nature Ptotocoles*, Vol. 5, no. 3, pp. 491-502, 2010

[42] LK. Fiddes, N. Raz, S. Srigunapalan, E. Tumarkan, CA. Simmons, AR. Wheeler, E. Kumacheva, “ A circular cross-section PDMS microfluidics system for replication of cardiovascular flow conditions”, *Biomaterials*, Vol. 31, no. 13, pp. 3459-64, 2010

[43] L. Chau, M. Doran, J. Cooper-White, “A novel multishear microdevice for studying cell mechanics”, *Lab chip*, Vol. 9, no. 13, pp. 1897-902, 2009

[44] M. Rossi, R. Lindken, B. P. Hierck, J. Westerwheel, “Tapered microfluidic chip for the study of biomechanical and mechanical response at subcellular level of endothelial cells to shear flow”, *Lab Chip*, Vol. 9, pp. 1403-1411, 2009

[45] JW. Song, W. Gu, N. Futai, K. A. Warner, JE. Nor, S. Takayama,” Computer-controlled microcirculatory support system for endothelial cell cuture and shearing” *Anal Chem*, Vol. 77, no. 13), pp. 3993-9, 2005

[46] J. Shao, L. Wu, J. Wu, Y. Zheng, H. Zhao, Q. Jin, J. Zhao, “Integrated microfluidic chip for endothelial cells culture and analysis exposed to a pulsatile and oscillatory shear stress”, *Lab Chip*, Vol. 9, no. 21, pp. 3118-25, 2009

[47] O.F. Khan, M. V. Sefton.” Endothelial cell behaviour within a microfluidic mimic of the flow channels of a modular tissue engineered construct”, *Journal of Biomedical microdevices*, Vol. 13, no. 1, pp. 69-87, 2011

[48] I, Barkefors. S, Le Jan, L. Jakobsson, E. Hejll, G. Calson, H. Johansson, J. Jarvius, JW. Park, N. Li Jeon, J. Kreuger, " Endothelial cell migration in stable gradients of vascular endothelial growth factor A and fibroblast growth factor2: effects on chemotaxis and chemokinesis" *J Biol Chem*, Vol. 283, no. 20, pp. 13905-12, 2008

[49] AD. Van Der meer, K. Vermeul, AA. Poot, J. Feijen, I. Vermes, " A microfluidic wound-healing assay for quantifying endothelial cell migration", *Am J Physiol Heart Circ Physiol*, Vol. 298, no. 2, pp. H719-25, 2010

[50] W. Cha, Y. Tung, M.E. Meyeroff, and S. Takayama, "Patterned electrode-based amperometric gas sensor for direct nitric oxide detection within microfluidic devices", *Anal Chem*, Vol. 82, no. 8, pp. 3300-3305, 2010

[51] D.M. Spence, N.J. Torrence, M.L. Kovarik, and R.S. Martin, " Amperometric determination of nitric oxide derived from pulmonary artery endothelial cells immobilized in a microchip channel", *Analyst*, Vol. 129, no. 11, pp. 995-1000, 2004

[52] T. D'Amico oblack, P. Root, and D.M. Spence, " Fluorescence monitoring of ATP-stimulated endothelium-derived nitric oxide production in channels of a poly(dimethylsiloxane)-based microfluidic device", *Anal. Chem*, Vol. 78, no.9, pp. 3193-3196, 2006

[53] M.Y. Rotenberg, E. Ruvinov, A. Armoza, S. Cohen, "A multi-shear perfusion bioreactor for investigating shear stress effects in endothelial cell constructs" *Lab chip*, Vol. 12, pp. 2696-2703, 2012

[54] X. Zhang, H. Li, Z. Ebin, S. Brodsky, M. Goligorsky, " Effects of homocysteine on endothelial nitric oxide production", A*merican Journal of Physiology*, Vol. 279, pp. 671-678, 2000

[55] A. Erol, M. G. Cinar, C. Can, M. Olukman, S. Ulker, S.Kosay, " Effect of homocysteine on nitric oxide production in coronary microvascular endothelial cells", *Endothelium*, Vol. 14, pp. 157-161, 2007

[56] E. Nagababu, J. M. Rifkind, "Measurement of plasma nitrite by chemiluminescence", *Methods Mol Biol*, Vol. 610, pp. 41-49, 2010

[57] Dow Corning, "Information about dow corning brand silicone encapsulants," online: http://www.dowcorning.com/applications/search/products/details.aspx?prod=01064291

[58] J. Shao, L. Wu, J. Wu, Y. Zheng, H. Zhao, Q. Jin, J. Zhao, "Integrated microfluidic chip for endothelial cells culture and analysis exposed to a pulsatile and oscillatory shear stress", *Lab ob a chip*, Vol. 21, pp. 3118-3125, 2009

[59] J. Liu, B. Cai, J. Zhu, G. Ding, X. Zhao. C. Yang, D. Chen, "Process research of high aspect ratio microstructure using SU-8 resist" *Microsystem Technologies*, Vol. 10, no. 4, pp. 265-268, 2004

[60] Microchem, “Nano SU-8 negative tone photoresist formulations 2025-2075 datahseet,” online: http://www.microchem.com/pdf/SU-82000DataSheet2025thru2075Ver4.pdf

[61] M. B. Chan-Park, J. Zhang, Y. Yehai, C.Y. Yue, “Fabrication of Large SU-8 Mold with High Aspect Ratio Microchannels by Uv Exposure Dose Reduction,” *Sensors and Actuators B: Chemical,* Vol. 101, pp. 175-182, 2004

[62] LM. Van Lerberge, K.M. Motsegood, D.J. Beebe, “ Three-dimentional micro-channel fabrication in polydimethylsiloxane (PDMS) elastomer” *Micromechanical system*, Vol. 9, no. 1, pp. 76-81, 2002

[63] R. Lima, S. Wada, S. Tanaka, M. Takeda, T. Ishikawa, K. Tsubota, Y. Imai, T. Yamaguchi, ” In vitro blood flow in arectangular PDMS microchannel: experimental observations using a confocal micro-PV system” *Biomedical microdevices*, Vol. 10, no. 2, pp. 153-167, 2008

[64] S. Hosseinpour, A.C. Liu, A.I. Barakat, J.C. Choy, B.L. Gray "Method of measuring nitric oxide release by vascular endothelial cells grown in microfluidic channels" *Proc SPIE 8976, Microfluidics, BioMEMS, and Medical Microsystems XII, 89761B*, 2014.

[65] GE water and process technology, “NOA liquid application” Online at http://www.geinstruments.com/products-and-services/nitric-oxide-analyzer/applications/noa-liquid-applications.html

[66] E. Nagababu, and J.M. Rifkind, “Measurement of Plasma Nitrite by Chemiluminescence” *Methods Mol Biol*, Vol. 610, pp. 41–49, 2010

[67] G. Rupert and Jr. Miller, “Beyond ANOVA-:Basics of Applied Statistics”, Fist edition, 1997 by Chapman&Hall

[68] R. Gould and C. N. Ryan, “Introductory Statistics; Exploring the World through Data”, 2013, Cloth Bonnd, 736 pages

[69] P.F. Davies,”Flow-mediated endothelial mechanotransduction”, *Physiol Rev*., Vol. 75, no. 3, pp. 519-560, 1995

[70] L. Kuruvilla, and C. Chandrasekharan Kartha, “Treatment with TNF-α or bacterial lipopolysaccharide attenuates endocardial endothelial cell-mediated stimulation of cardiac fibroblasts”, *Biomed Sci*, Vol.16, no. 1, pp. 16-21, 2009